

Signal Identification for Visual Electrophysiology

A comparison of signal analysis techniques and their
application to clinical electrophysiology of vision.



UNIVERSITY OF
GOTHENBURG

Thomas Wright

Institute of Neuroscience and Physiology

at Sahlgrenska Academy

Gothenburg

2012

Signal Identification for Visual Electrophysiology

A comparison of signal analysis techniques and their application to clinical electrophysiology of vision.

Thomas Wright, Institute of Neuroscience and Physiology at Sahlgrenska Academy, University of Gothenburg, Göteborg, Sweden, 2012

Aims: The aim of this thesis was to investigate the use of objective methods for the analysis of visual electrophysiological recordings. Specifically can signal identification algorithms identify electrophysiological signals and can they be applied to improve clinical testing and analysis?

Methods: Automated signal identification algorithms were applied to multifocal electroretinogram (mfERG) and visual evoked potential (VEP) recordings. To simulate the types of signal identification problems encountered in the clinical environment, recordings were performed on healthy volunteers then artificially modified to represent the effects of disease. A multivariate analysis, spatial-temporal partial least squares (st-PLS) was applied to mfERGs recorded from a population of patients with Type 1 diabetes.

Results: Signal identification algorithms were able to identify mfERG and VEP responses that had been artificially attenuated. The best performing algorithms outperformed human expert observers at identifying preserved mfERG responses. Application of signal detection algorithms increased the quality and reduced the time for recording VEPs. Metrics of algorithm performance demonstrated that algorithms using more prior knowledge about expected waveform morphology performed better than algorithms that were naive. Changes to retinal function in patients with Type 1 diabetes, measured using the mfERG, were detected using st-PLS analysis. The st-PLS analysis revealed information about the spatial and temporal distribution of these changes that was not revealed using traditional analysis methods.

Conclusions: The application of more advanced analytical techniques can increase the accuracy and decrease the time required for clinical testing. Multivariate analysis techniques can reveal novel information about disease etiology.

Key-words: Visual Electrophysiology, Signal detection, Signal-to-Noise Ratio, multivariate analysis, spatial-temporal partial least-squares

Original articles

This work is based on the following articles:

- I. Wright, T., Nilsson, J., Gerth, C., Westall, C. 2008. A Comparison of Signal Detection Techniques in the Multifocal Electroretinogram. *Documenta Ophthalmologica*. 117(2):163-70
- II. Wright, T., Nilsson, J., Westall, C. 2011. Isolating Visual Evoked Responses: Comparing Signal Identification Algorithms. *Journal Of Clinical Neurophysiology*. 28(4):404-411
- III. Wright, T., Cortese, F., Nilsson, J., Westall, C. 2012. Analysis of multifocal electroretinograms from a population with type 1 diabetes using partial least squares. *Documenta Ophthalmologica*. In Press.

All papers are reproduced with permission from the publishers.

Abbreviations

cd	Candela
CRT	Cathode Ray Tube
CSNB	Congenital Stationary Night Blindness
EEG	Electro-encephalogram
EOG	Electrooculogram
ERG	Electroretinogram (Electroretinography)
mfERG	Multifocal Electroretinogram
sf-mfERG	Slow-flash Multifocal Electroretinogram
ERP	Early Receptor Potential
ERP	Event-related Potential
ICA	Independent Component Analysis
IPL	Inner Plexiform Layer
ipRGC	Intrinsically Photosensitive Retinal Ganglion Cell
ISCEV	International Society for Clinical Electrophysiology of Vision
LGN	Lateral Geniculate Nucleus
MAR	Minutes Of Arc
OA	Ocular Albinism
OC	Optic Chiasm
OCA	Ocular-cutaneous Albinism
OP	Oscillatory Potentials
OPL	Outer Plexiform Layer
PCA	Principal Component Analysis
PhNR	Photopic Negative Response
PLS	Partial Least-squares
st-PLS	Spatio-temporal Partial Least Squares
RMS	Root Mean Squared

RP	Retinitis Pigmentosa
RPE	Retinal Pigment Epithelium
STGD	Stargardt Macular Dystrophy
SNR	Signal-to-noise Ratio
VEP	Visual Evoked Potential

Table of Contents

Original articles.....	iii
Abbreviations.....	v
Introduction.....	1
The visual pathway.....	4
Structure of the retina.....	5
Retinal Function.....	8
Cortical Visual System.....	11
Visual Electrophysiological Methods.....	15
Retinal Electrophysiology.....	15
Multifocal Electroretinogram.....	17
Electrode choice for electroretinograms.....	20
Visual Evoked Potentials.....	20
Clinical Electrophysiology of Vision.....	23
The normal electroretinogram.....	23
The normal multifocal electroretinogram.....	25
The normal visual evoked potential.....	26
Diseases of the retina.....	27
Rod photoreceptor dominated disease.....	27
Cone photoreceptor dominated disease.....	29
Middle retina disease: X-linked Congenital Stationary Night Blindness.....	30
Diseases affecting the cerebral visual system.....	33
Ocular Albinism.....	33
Assessing Visual Acuity with the visual evoked potential.....	36
Optic Neuritis.....	37
Summary.....	38
Signal Analysis.....	40
Signal extraction in the frequency domain.....	42
Signal extraction in the time domain.....	44
Analyzing waveforms in the time domain.....	46
Measuring signal quality.....	47
Objectives.....	49
Specific objectives and aims.....	49
Paper I.....	49
Paper II.....	49
Paper III.....	49
Methods.....	50

Recording protocols.....	50
Multifocal Electroretinogram (mfERG) Paper I & III.....	50
Visual Evoked Potentials (VEP) Paper II.....	51
Simulating the effects of disease.....	51
Paper I.....	52
Paper II.....	53
Signal detection algorithms.....	53
Paper I.....	53
Paper II.....	53
Measuring Performance.....	54
Paper I.....	54
Paper II.....	54
Identifying changes to retinal function occurring as a result of disease	
.....	54
Paper III.....	54
Results and Discussion.....	56
Signal detection algorithms.....	56
Effect of increasing noise.....	56
Effect of prior knowledge.....	59
Identifying changes due to disease.....	60
Limitations.....	63
Conclusions.....	65
Paper I.....	65
Paper II.....	65
Paper III.....	65
Summary.....	66
Acknowledgements.....	67
References.....	68

Introduction

The human visual system is a masterpiece of evolution that enables us to perceive the existence, form and location of objects in our local environment. The interaction of multiple cell types in specialised structures and pathways allows visual perception over a huge dynamic range. Human vision can operate both in very dim light (10^{-6} candela (cd)) and very bright (10 cd), a 14 log unit range (Hood & Finkelstein 1986). It is sensitive to wavelengths (colour) from $< 400\text{nm}$ to $> 650\text{nm}$ and is able to differentiate changes of between 2 and 10 nm (Foley J.D. et al. 1996). The ability to differentiate between two lines positioned close together (visual acuity), has been shown to be < 1 minute of arc (MAR) in emmetropic eyes with the potential for < 0.5 MAR (Rossi et al. 2007).

Human vision is much more than the simple detection of the presence or absence of light. Multiple metrics can be used to measure visual performance and experimentation has demonstrated non-linear relationships between the different measures. Visual information requires multiple stages of processing, both in the retina and the cortex, to allow us to form the rich representation of our environment that is referred to as visual perception. This processing takes place in a generally hierarchical manner, moving from simple to complex as the visual information is passed from the eye through the visual pathways in the brain.

Electrophysiology is the study of electrical potentials generated by biological processes. The function of many cellular processes is dependent on the balance of positive and negative ions across cellular membranes. There are many techniques that have been used to record these changes in electrical potentials operating at a range of scales. Potentials have been recorded from single ion channels, single cells as well as entire organs. Clinical visual electrophysiology concentrates on non-invasive recordings of electrical potentials from the eye and the primary visual cortex. The relative accessibility of these organs aids the process of recording.

Clinical visual electrophysiology can be categorized into two main techniques.

Electroretinography (ERG) records the electrical potentials generated in the retina in response to stimulation with light. Electrical potentials generated in the retina are conducted through the eye and are detected using an electrode placed on (or close to) the front of the eye (cornea). By modifying the adaptation state of the eye and the composition of the stimulus different retinal cell types can be targeted. As different cell types in the retina are activated a complex waveform can be recorded. A sub type of the electroretinogram is the multifocal electroretinogram (mfERG), this involves stimulating, and isolating responses from multiple retinal regions. The mfERG allows retinal responses to be visualised as a topographic map of retinal function. Visual evoked potentials (VEP) record the electrical potentials generated in the primary visual cortex. Typically electrodes are placed on the surface of the scalp over the visual cortex (V1). The visual signal must be detected by the retina and then transduced via the optic nerves before reaching the visual cortex and being detected by the recording electrodes. Abnormalities occurring anywhere in this pathway will modify the final recorded waveform. In addition to electroretinography and visual evoked potentials other techniques such as the electrooculogram (EOG) are used.

A common problem affecting all electrophysiological techniques is that of signal detection. Particularly in techniques used in clinical electrophysiology the amplitude changes of the electrical potentials of interest are relatively small requiring external amplification for visualization. When the amplification is performed without using any prior knowledge about the signal of interest it is generic, equally amplifying all electrical potentials detected by the sensing electrodes. Typically this will include electrical potentials generated by other biological processes, such as muscle contractions or background brain activity, as well as any electrical potentials generated by sources external to the body.

This work examines how using prior knowledge about the expected response potentials can be used to improve the identification and characterizations of responses. Techniques are applied to both multifocal electroretinograms (Papers I & III) and visual evoked potentials (Paper II). A difficulty common to these types of studies is how to measure improvement in the absence of knowledge about the true underlying signal. Methods are introduced that artificially manipulate the electrophysiological recordings in a well characterized manner

T. Wright Signal detection in clinical visual electrophysiology

(Papers I & II) to determine the performance of signal detection techniques.

The visual pathway

The most obvious organs involved in vision are the eyes. Often represented as a simple globe, the human eye is made up from multiple structures. These structures have many roles supporting and enhancing the ability of the retina to detect light, dark and form. These include muscles and nerves that control motility, structures that can change the optical properties of the system such as the pupil, which controls the total amount of light being allowed to enter the eye, and the cornea and lens which can adjust the focal length.

Arguably the most fundamental structure of the eye is the retina. In many simple organisms the differentiation of light and dark may be the only perception possible. The only requirement for this purpose is a light sensitive neuron, which is exposed to the external environment (von Helmholtz 1909). In the human eye the structure of the retina is much more complex, thus allowing significant amounts of visual processing to take place.

The retina forms a complex layered structure with multiple cell types (Figure 1). There are several cell types involved in the detection, processing and transmission of the visual signal. Other, non-neuronal cells, such as Müller cells support the function and regeneration of the retinal circuitry.

The mammalian retina is supplied with blood from two main sources. The majority of blood flow comes from arteries in the outer choroid. This blood flow supports the outer layers of the retina including the retinal pigmented epithelium and the photoreceptors. A separate artery, the central retinal artery passes into the eyeball at the optic nerve head, this artery forms a network on the inner surface of the retina to supply the neural structures of the inner retina (Cioffi et al. 2003).

Structure of the retina

The basal layer of the human retina is the retinal pigmented epithelium (RPE). This single layer of cells sits between the blood supply of the choroid and the outer segments of the photoreceptors. The cells of the RPE are heavily pigmented and have a role in improving the optics of the eye by absorbing scattered light. There is a strong interdependence between the photoreceptors and RPE, the RPE is necessary to support the function of the photoreceptors. The next retinal layer is formed by the photoreceptors, in the human retina there are four types of photoreceptors. Cone photoreceptors are classified according to the wavelength of light, short (S-cones), medium (M-cones) or long (L-cones) that they are maximally sensitive too. The fourth type of photoreceptor (rods) are highly sensitive at low light levels. All photoreceptors have a similar structure consisting of two parts, an inner and an outer segment connected by a thin cilium. The tips of the outer segments are embedded in the RPE, they contain a stack of flattened disks of membrane containing molecules of the visual pigments (opsins). The inner segment of the photoreceptor contains the structures involved in maintaining the cell, including a large number for mitochondria to generate the energy required for photo-transduction. The structure of the outer segment differs between the two major classes of photoreceptor. In the rod photoreceptors the membrane disks are tightly packed in a long column. This maximizes the change of a photon intercepting the photo-pigment maximizing the sensitivity of this cell type to light. In the cone photoreceptor the membrane disks are more spread out providing a larger surface area and allowing faster transfer of substances required to regenerate the cell after stimulation by light. This difference in structure leads to a difference in morphology with cones appearing shorter and fatter than rods (Burns & Lamb 2004).

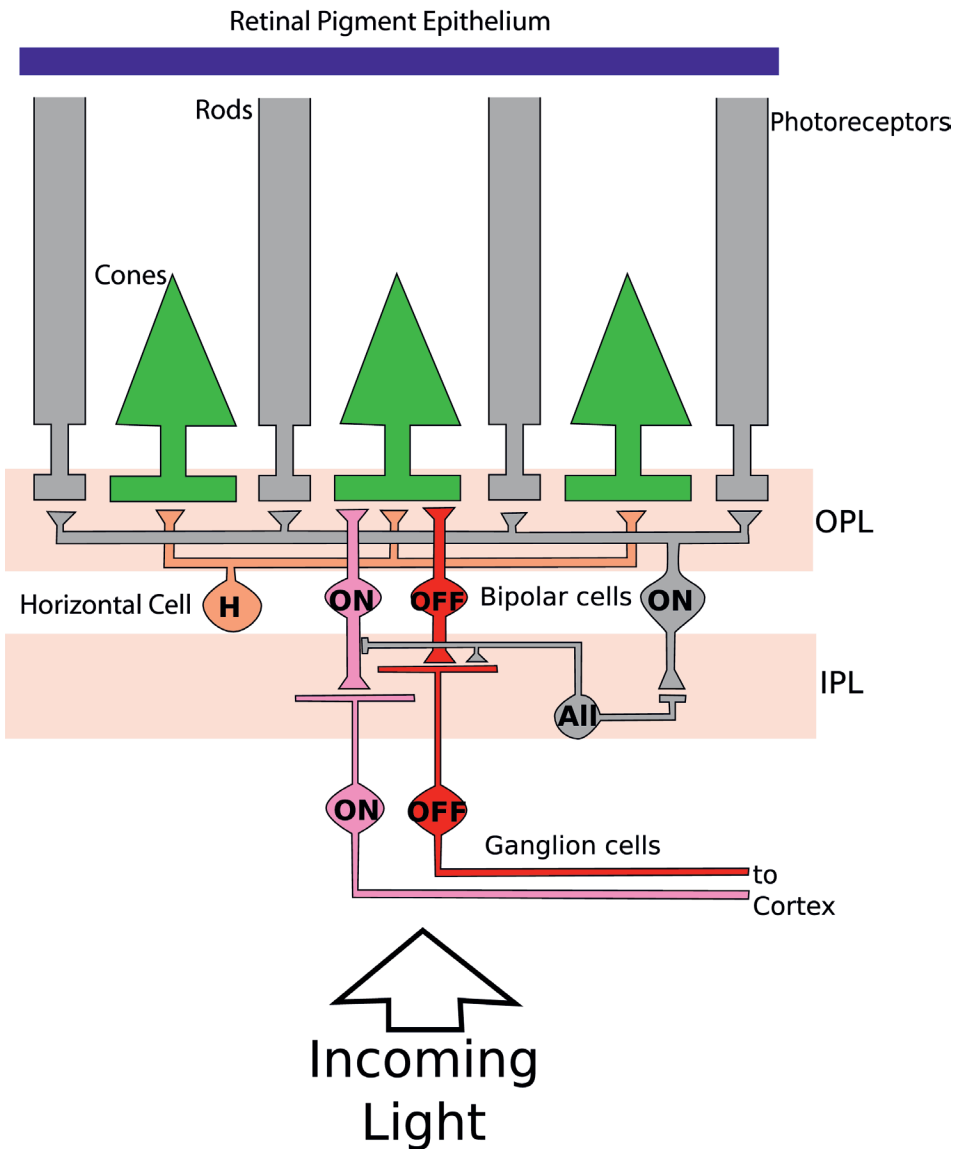


Figure 1: Retinal connectivity. Schematic diagram showing neuronal cell types of the mammalian retina. OPL outer plexiform layer, IPL inner plexiform layer. Image modified with permission from (Schiller 2010).

The inner segments of both rods and cones terminate in a synaptic junction. These synaptic junctions interface the photoreceptors with a complex neuronal network. The initial connection with this network is to a family of cells referred

to as bipolar cells. At least 10 different bipolar cells have currently been identified (Dacey 1999), these cells differ in both morphology and function. Functionally the bipolars are classified according to whether they respond when the stimulating photoreceptors detect an increase in light intensity (ON-bipolars) or a decrease in relative light intensity (OFF-bipolars). Morphologically the bipolar cells are classified according to the types of photoreceptors, rods or cones that they connect to, the number of photoreceptors that they connect to and the depth in the retina of their terminal connections (Masland 2001). In general cone midget bipolar cells synapse with only a few cone photoreceptors, but in the fovea a midget bipolar cell will synapse with a single cone. Diffuse bipolar cells form synapses with multiple photoreceptors and can spread over relatively large retinal areas. The receptive fields (the retinal area covered by a single bipolar cell) can vary greatly in size from $< 1^\circ$ visual angle to $> 10^\circ$. That diffuse bipolar cells interface with multiple photoreceptors allows for integration of the stimulus from multiple photoreceptors. Electrophysiological recordings performed by inserting an electrode into a single cell have shown that bipolar cells have a centre surround organisation where stimulation of photoreceptors connecting to the periphery of a receptive field have an antagonistic response to the response to photoreceptors connecting closer to the centre (Lukasiewicz 2005). This centre surround organisation provides a mechanism for basic visual processing such as edge detection and colour perception (Jacobs 1969).

In turn the bipolar cells interface with a family of ganglion cells. 20-25 anatomically different types of ganglion cells have been identified and again these are classified according to the size of their visual field and the retinal depth where they synapse with the bipolar cells. The ganglion cells traverse the inner surface of the retina to where they exit the eye at the optic nerve head. From the eye these ganglion cells pass the retinal signals to multiple distinct targets in the midbrain and thalamus of the brain (Masland 2001).

To further complicate the retinal circuitry the interactions between photoreceptors and bipolar cells are modulated by horizontal cells. Horizontal cells synapse with multiple photoreceptors and form gap junctions with each other. They provide a negative feedback signal to photoreceptors and as a result are important in generating the visual fields of both bipolar cells and ganglion

cells. The connections between bipolar cells and ganglion cells are also modulated by another family of amacrine cells. It is estimated that there are at least 40 different types of amacrine cells in the primate retina (Dacey 1999).

As can be seen from the complex circuitry within the retina the common model of the retina as a photographic film is overly simple. Far from just detecting the presence or absence of light the retina is capable of considerable visual processing.

Retinal Function

When the photoreceptor is not stimulated by light there is a steady current, 'the dark current' of mainly sodium ions flowing through the cell membrane. The ions enter the cell through cyclic guanosine monophosphate (cGMP) channels in the outer segment membranes. In the dark this current holds the cell in a partially depolarised state. This leads to the constant release of glutamate, a neural transmitter. When a photon of light interacts with the opsin complex in the outer segment of the photoreceptor the opsin molecule is isomerised to an active form initiating a protein cascade that leads to the closing of the cGMP channels. As the positive charged sodium ions cannot enter the cell this leads to the photoreceptor hyperpolarising and the release of glutamate is stopped.

The decrease in glutamate at the synapse between the photoreceptor and the bipolar cell can have differing effects according to the particular type of bipolar cell. The decrease in glutamate causes ON-bipolar cells to become more positive (depolarised) while the opposite response (hyper-polarisation) occurs in OFF-bipolar cells. These two opposite responses are mediated by two different types of glutamate receptor. OFF-bipolar cells express direct ionotropic glutamate receptors, two types of ionotropic receptors have been observed in bipolar cells; AMPA and kainate. Both these receptors form direct ion channels through the cell membrane allowing the passage of cations such as calcium, sodium and potassium when the receptor is activated by the presence of glutamate. Thus OFF-bipolar cells are held in a slightly depolarised state when glutamate is released by the photoreceptors (i.e. in the dark), once the glutamate

release is reduced (i.e. in the presence of light) the influx of cations to the bipolar cell is stopped and the cell hyperpolarises (Smith 2006).

ON-bipolar cells show a reversal in response, becoming depolarised in the absence of glutamate. This response is mediated by indirect metabotropic glutamate receptors. One such receptor that has been characterised in the retina is the 2-amino-4-phosphonobutyric acid (APB) receptor. When the APB receptor is activated in the presence of glutamate an intracellular signaling cascade closes ion channels permeable to cations causing the bipolar cell to hyperpolarise (Nelson & Connaughton 1995; Slaughter & Miller 1981).

The horizontal cells mediate interactions between multiple photoreceptors. They consist of a central cell body surrounded by an electrically isolated axonal arbour. The primary functional role of the horizontal cells is a negative feedback pathway suppressing the activation of connected cone photoreceptors. The exact mechanism of this feedback is not yet clear, initially it was thought to be dependent on the release of GABA, however other studies have implicated a GABA independent pathway that modulates the Ca^{2+} current in the cone photoreceptors (Fahrenfort et al. 2005; Kamermans & Spekreijse 1999). The horizontal cells show spatial organisation of their inputs, thus hyperpolarisation of the photoreceptors synapsing with the periphery of the horizontal cell modulates the Ca^{2+} flow in the synapse of cones synapsing close to the horizontal cell body, decreasing their sensitivity to changes in luminance (Kamermans & Spekreijse 1999; Verweij et al. 1996).

Like the photoreceptors, the bipolar cells also release glutamate as their neurotransmitter. The ON and OFF cone bipolar cells synapse directly with ON and OFF ganglion cells. Rod bipolar cells synapse almost exclusively with amacrine cells. Input from rod ON-bipolar cells is passed via the amacrine cells to a cone ON-bipolar, ganglion cell synapse. The rod OFF signal is in turn passed via the amacrine cell, with a signal inversion, reducing glutamate release to a cone OFF-bipolar cell stimulating a cone OFF-ganglion cell (Nelson 1982; Kolb 1997). The amacrine cells are extensively coupled by gap junctions, these are highly dependent on the state of light or dark adaptation in the retina. The amacrine cells form feedback synapses with bipolar cells allowing them to act

in a similar fashion to the horizontal cells, mediating lateral interactions between the bipolar cells. Both amacrine and ganglion cells respond to excitation by forming action potentials. The action potentials from amacrine cells can either be sustained, responding to a change in light with a maintained discharge, or transient, firing at light onset or offset (Kolb 1997).

As can be seen, unlike the majority of neurons in the nervous system, the photoreceptor and bipolar cells act in an analogue manner showing a gradient of responses. Once the bipolar cells synapse with the retinal ganglion cells the retinal visual system takes on a binary nature. The action potentials of ganglion cells show complex patterns in response to stimulation. Some ganglion cells show a center surround organization of the receptive field, and On-centre retinal ganglion cell shows increased activity when light stimulates the centre of its receptive field, when light stimulates the periphery of the visual field it will respond by decreasing the rate of action potential generation, when both the center and surround receptive fields are illuminated the effects cancel out and the rate of action potential generation remains unchanged. Other ganglion cells have been shown to be activated (or suppressed) by lights moving in a preferred direction, or by edges (sharp changes in light intensity) across the receptive field (Falk & Shells 2006). Recent research has identified a new class of ganglion cells, the intrinsically photosensitive retinal ganglion cells (ipRGC), which contain the photo-pigment melanopsin. These ipRGCs are not thought to be involved in vision but instead play a role in circadian rhythms and the pupillary light reflex (Schmidt et al. 2011).

Cortical Visual System

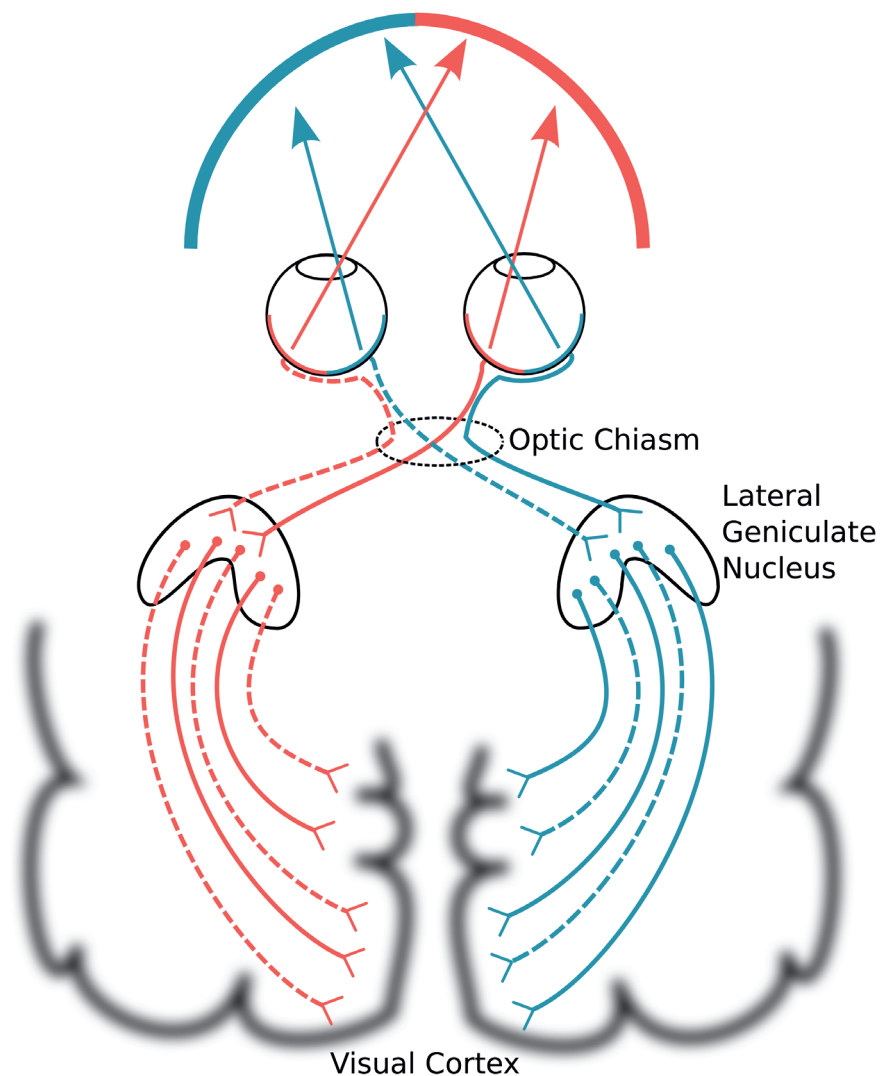


Figure 2: Schematic representation of the cortical visual pathways. Neurons from the nasal retina cross at the optic chiasm. The first synapse for retinal ganglion cells is in the Lateral Geniculate Nucleus. Inputs from each eye are segregated until they terminate in V1.

The final cell type in the retina is the retinal ganglion cell. The axons of these neurons pass over the inner surface of the retina forming the retinal nerve fibre layer and converge at the optic nerve head, here they exit the retina forming the optic nerve. The optic nerves of the two eyes converge at the optic chiasm (OC). At the OC some of the axons from the two eyes undergo decussation, axons originating in the nasal retina cross sides so the left half of the visual field is perceived by the right cerebral hemisphere and vice versa. As axons originating in the temporal retina are carrying information about the opposite side of the visual field (i.e. Temporal retina in the left eye encodes information from the right side of the field of view) there is no need for these axons to cross over (Figure 2). The first synaptic terminal for the majority of the retinal ganglion cells is in the Lateral Geniculate Nucleus (LGN) in the thalamus. After synapsing in the LGN the visual information passes, via the optic radiations, to the primary visual cortex. Connections have been identified from the primary visual cortex projecting to many distinct cortical regions involved in aspects of higher order visual processing (Figure 3).

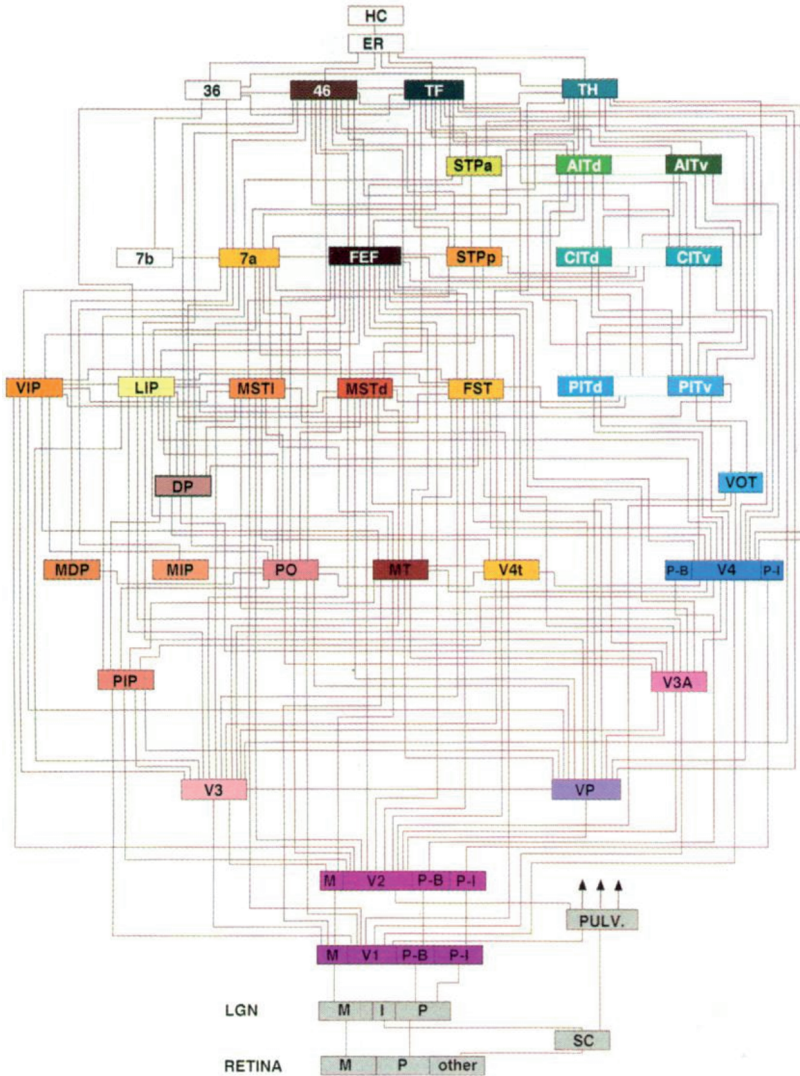


Figure 3: Cortical regions involved in vision. Map showing connectivity between cortical areas of vision in the macaque. Reproduced with permission from (Van Essen et al. 1992).

This should not be interpreted as indicating that the flow of visual information is linear and uni-directional. Even in the early parts of the visual pathway feed back connections form a significant proportion of the neural synapses. In the LGN it is estimated that only 10% of the neurons are afferent from the retina while 30% of the neurons are feed-back from other cortical regions (Sherman 2001).

The primary destination for visual information from the LGN is the primary visual cortex (V1), this is located in the posterior pole and along the Calcarine Fissure on the medial sides of the occipital lobes of the brain (Figure 4). Early anatomical studies recognized that the visual cortex was made up of several layers, a commonly used numbering scheme was proposed by Brodmann in 1909 (Garey 2006) which divided the visual cortex into 6 layers. Layer 1 (most dorsal) has very few neurons, layers 2 & 3 have many excitatory neurons that connect to other cortical areas involved in visual processing. The axons projecting from the LGN terminate in layer 4 of the visual cortex. Finally layers 5 & 6 have axonal projections that provide feedback circuits to the LGN. Studies injecting a radioactive marker, that is taken up by, and transported along neurons, showed that the axonal terminals in layer 4 segregate according to the eye of origin (Wiesel et al. 1974). In addition to the formation of ocular dominance columns, axons from similar retinal areas project to similar locations in V1, leading to the formation of a retinotopic map with regions of the visual cortex representing regions of the retina (Figure 4). As the density of photoreceptors and ganglion cells is greatest in the centre of the retina (the fovea), the equivalent area of V1 is proportionally larger than that representing more peripheral retina.

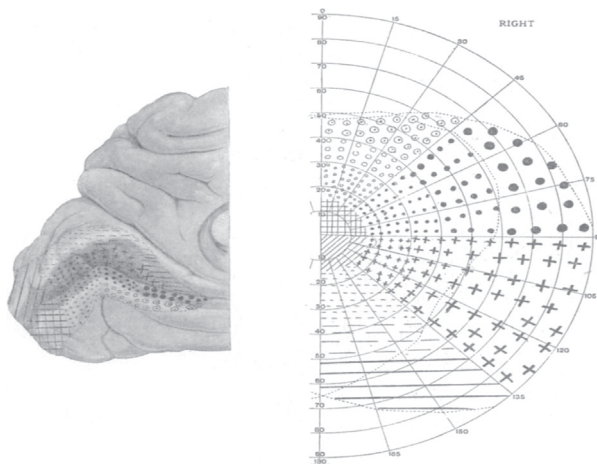


Figure 4: Retinotopic map of the human visual cortex. *Left: The striate area of the left hemisphere of the brain is shown with the Calcarine Fissure opened to reveal the internal portion. Right: The right half of one visual field. The markings represent the different segments of the visual field on the cortex. Reproduced from (Holmes 1945).*

Visual Electrophysiological Methods

Retinal Electrophysiology

The activation of neuronal cells in the retina gives rise to changes in the electrical potential of the eye. Using electrodes placed close to the eye these electrical potentials can be measured. The resultant waveforms of electrical potential against time are complex with different neuronal generators overlapping with positive and negative potentials. An early analysis of the mammalian ERG recorded from cats, suggested that it was formed by the summation of three separate potentials termed PI, PII and PIII (Granit 1933) (Figure 5). Since these early recordings technological developments have allowed the identification of many smaller potentials (Figure 6).

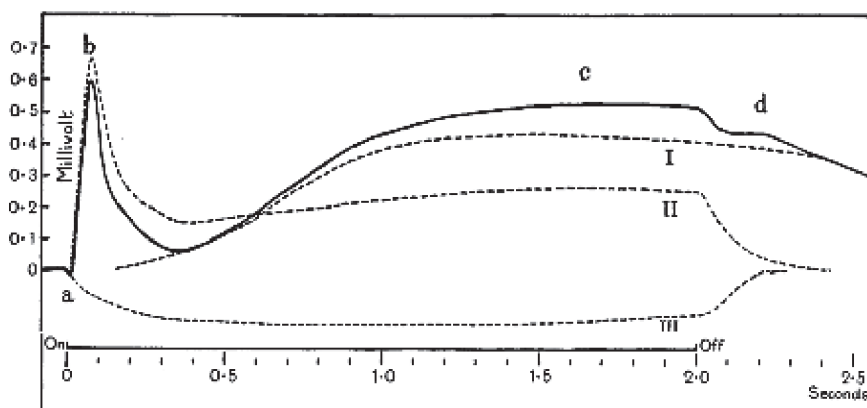


Figure 5: Components forming the retinal action potential. Early recordings of the retinal action potential identified 4 components (termed a,b,c and d-waves). It was suggested these were formed by the summation of 3 separate potentials (PI, PII and PIII). Components: broken lines, Composite curve drawn in full. The a-wave is broadened slightly out of scale to show its derivation more clearly. Reproduced from (Granit 1933).

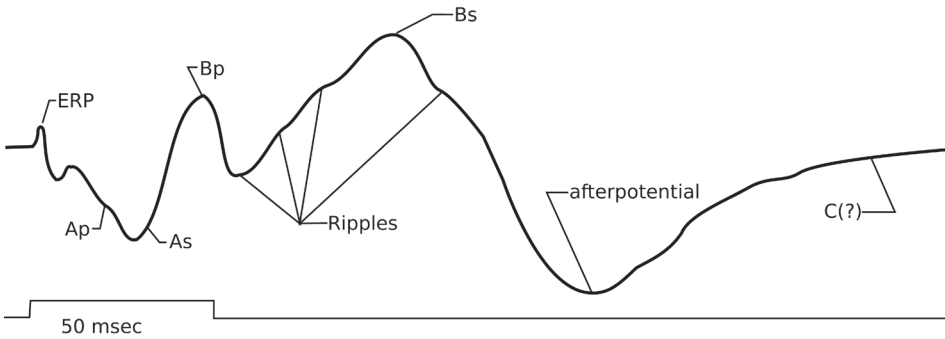


Figure 6: Components of the human electroretinogram. An idealised ERG waveform showing the early receptor potential (ERP), the photopic and scotopic a waves (Ap and As), the photopic and scotopic b waves (Bp and Bs), the late negative response (afterpotential), and the C wave. Ripples occur throughout the entire response. Not all the components shown are seen in any single recording condition. Reproduced from (Armington 1974).

The primary components of the ERG that are of interest in a clinical analysis are the a-wave and the b-wave. In a dark adapted eye the response to a low intensity flash does not have a significant a-wave component, however as the flash intensity increases the a-wave becomes more prominent. The negative a-wave represents the leading edge of Granits PIII component and is due to the relative increase in sodium ions in the extra-cellular matrix as the photoreceptors hyperpolarise in response to light. As the visual signal is transmitted along the retinal pathway to the bipolar cells they depolarise, releasing potassium ions. These ions are taken up by Müller cells, which span the entire depth of the retina and it is thought that it is currents originating in the Müller cells that gives rise to the positive going b-wave (Kline et al. 1978). More recent research has indicated that current in the Müller cells may not be the sole origin of the b-wave and that ON-center bipolar cells as well as ganglion cell activity may also contribute (Lei & Perlman 1999). High frequency oscillations can be observed on the rising edge of the b-wave, while the exact origins of these oscillatory potentials (OPs) is not clear, it is likely they do not have a single origin. The early OPs probably originate from the cone pathway while the later OPs represent processes of the rod pathway (Rousseau & Lachapelle 1999). Animal studies have indicated that the OPs directly represent the activities of the neuronal bipolar and amacrine cells (Wachtmeister 1987). Other potentials that may have clinical use include the d-

wave and photopic negative response (PhNR). The d-wave is visible only when the stimulus is of a long (>100 ms) duration and is thought to represent response of the off-bipolar cells (Xu & Karwoski 1995). The PhNR is a negative potential occurring after the b-wave. It can be optimized by using stimuli that preferentially target a single class of cone photoreceptor (Rangaswamy et al. 2007). The response is thought to represent the glial cell response to activation of the retinal ganglion cells (Viswanathan et al. 1999).

Multifocal Electroretinogram

As described earlier the ERG uses an electrode placed on the cornea to record the gross retinal response to stimulation by light. Useful information can be obtained by modifying the stimulus intensity, colour and frequency and by changing the adaptation state of the retina. In all cases however, the light stimulation is designed to give homogeneous illumination of the retina. Because there is only a single input (the light) and output is only recorded from a single electrode the full field ERG method it is not possible to infer any information about the topographic distribution of the ERG potentials from the retina and localised regions of retinal dysfunction can be obscured by the response from the rest of the healthy retina. This is particularly significant when the regions of retinal dysfunction are localised to the macular, since small regions of dysfunction here may have significant effects on vision. Before the development of the multifocal ERG, information about the spatial distribution of retinal responses was obtained by using small, focal stimuli, as the generated retinal response is correspondingly small long recording times are required to derive the retinal response. These long recording times preclude obtaining responses from many retinal areas using this method. Comparing responses from multiple retinal regions becomes difficult due to variations within the recording session and between multiple sessions.

The multifocal electroretinogram (mfERG) technique was introduced in 1991 by E. Sutter (Sutter & Tran 1992) to address this problem. The multifocal technique depends on the simultaneous stimulation of multiple retinal areas. The gross retinal response is recorded using a single electrode. Individual responses from each stimulated area are extracted post recording using a mathematical algorithm. In order for this extraction to be successful each individual stimulation element must be independent of all the others. A common

way of ensuring this independence is to control the elements of the visual stimulus, using a maximum length sequence (m-sequence). The m-sequence is simply a binary number of length 2^n-1 where $n >$ number of hexagons in the array (e.g. 1001110 is an m sequence of length 2^3-1). M-sequence numbers have properties that make them suitable for the purpose of driving a multifocal ERG stimulus. In particular they have a uniform distribution of the 1s and 0s through the sequence, also the values in the sequence are independent; no value can be predicted from the other values. If an m-sequence is shifted by any number of places the resultant sequence has zero correlation with the original m-sequence. This allows each element in the stimulus array to be controlled by the same m-sequence shifted by a number of places. The response from each stimulus element can then be extracted by adding all the trials in which the stimulus element was activated and subtracting all the trials in which the element was inactive. The extraction of responses from the mfERG is very flexible, the most normal extracted response is that of a single flash of each element (1st order kernel), it is also possible to extract response from other combinations of element stimulation. For example responses in which a single element has been stimulated twice in succession (2nd order, 1st slice), this response represents retinal adaptation to a preceding flash (Sutter 2001) (Figure 7).

There are several different commercially available multifocal electroretinography systems. All recordings in this work were performed using the Veris™ multifocal system (Electro-diagnostic Imaging, Redwood City, CA, USA). The stimulus for the Veris system consists of an array of hexagons, the experiments in this work used stimulus arrays of 61 or 103 elements but arrays with more or less elements are available. Optionally the stimulus hexagons can be scaled to approximate the size of the retinal response from different retinal areas, i.e. hexagons in the centre of the array are smaller than hexagons in the periphery; this allows greater detail to be gathered from the central retina where the cone density is highest. The stimulus is generated using a small 2" cathode ray tube (CRT), optical magnification is used so the stimulus subtends ~40° of the retina. Obviously a key requirement for accurate spatial mapping of retinal function is accurate placement of the stimulus on the retina. The Veris system aids stimulus placement with a camera operating at infra-red wavelengths, which can visualize the fundus as the stimulus is presented. This fundus image can also be used to monitor fixation during recordings.

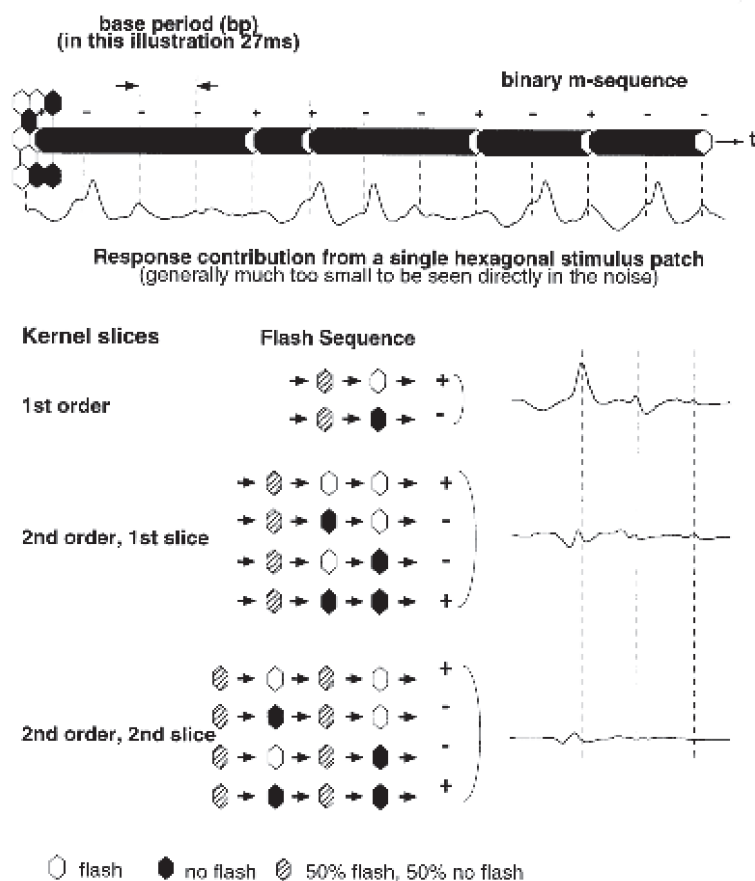


Figure 7: Extracting responses from the multifocal m-sequence. Top shows a representation of m-sequence stimulation from 1 hexagon. The trace below represents the corresponding sequence from the same hexagon. The derivation of 1st and 2nd order responses is shown below. Reproduced with permission from (Sutter 2001).

Electrode choice for electroretinograms

There are many different types of electrodes that have been used for recording ERGs and mfERGs. All electrodes require placing a conductive material as close as possible to the neural elements that are generating the electrical potentials of interest. The electrical potentials are conducted from the retinal generator sites, through the intervening tissues to the conductive element of the electrode (Coupland 2006). Changes to the electrical potentials of the active electrode are detected by comparison with a second electrode, the reference electrode. The reference electrode is positioned so as not to be affected by potentials from the retinal generating sites of interest. Often the reference electrode is placed in the contra-lateral eye when monocular stimulation is performed. Electrodes placed on the ear-lobes, the outer canthus or forehead are also used. Many studies have shown that the type and position of both the active and recording electrodes can have a significant impact on the recorded potentials (Odom et al. 1987; Mentzer et al. 2005). In the studies described in this work the bipolar Burian-Allen (Hansen Ophthalmic Laboratories, Iowa City) contact lens electrode was used. This electrode consists of a clear corneal contact lens that is held against the cornea by a spring assembly. The contact lens is surrounded by a circular silver wire that acts as the active electrode. The lens is mounted inside a speculum that holds the eyelids apart and contacts with the scleral surface. The outer surface of the electrode is coated with silver and acts as the reference electrode. Use of the Burian-Allen lens has a small risk of corneal abrasion and moderate discomfort; however it is tolerated well by most people. Due to the stable configuration of the active and reference electrodes it consistently gives a good signal-to-noise ratio (SNR) and consistent recordings (Lawwill & Burian 1966).

Visual Evoked Potentials

The location of the visual cortex is fortuitous for electrophysiologists interested in studying its electrical activity. The visual cortex is located close enough to the skull that electrodes can be placed on the scalp and electrical potentials occurring in the cortex can be recorded. Due to the retinotopic layout of the visual cortex, however, inputs projecting from the macular region of the retina project to the occipital pole while inputs from more peripheral retina project to cortical areas deeper inside the Calcarine fissure. The position of electrodes

placed on the scalp mean that the VEP is dominated by stimulation of the central retina and is relatively insensitive to stimulation of the peripheral retina. Typically an active electrode is placed over the occipital cortex in location Oz defined by the International Standard 10-20 EEG System (Jasper 1958). The scalp location is cleaned using mild abrasion and the electrode is embedded in a conductive paste or gel to ensure a good connection. A reference electrode is placed in a separate location that will not be influenced by activity in the visual cortex. Location Fz or an earlobe is often used. If information is required about the differential functioning of the cortical hemispheres, additional electrodes can be placed over each cortex. Locations O1 and O2 and PO7 and PO8 are often used for this purpose (Odom et al. 2010).

The brain is not a quiet organ and electrical potentials are constantly being generated. Typically the electrical potentials evoked in the visual cortex in response to visual stimulation are of a similar, or smaller, magnitude to the other concurrent potentials, thus multiple repetitions of the visual stimulation is required and the signal is extracted using averaging. Clinical recommendations indicate this process should be repeated at least twice for each response to demonstrate repeatability.

A system for recording the VEP consists of a stimulus presentation system, often a computer linked to a colour or monochrome monitor and a signal amplifier and recording system, usually a computer with an analog to digital conversion board. A key requirement of the recording system is that it can average together signals accurately time-locked to the stimulus presentation. All recordings presented in this work were performed using a commercially available NuAmps system with Scan2 software (Compumedics Neuroscan, Charlotte, NC, USA) for recording, with a computer running StimulusMaker™ (Vision Research Graphics Inc., Durham, NH, USA) for the stimulus presentation.

Many different visual stimuli can be used to evoke the VEP. Unstructured flashes of light can be presented either monocularly or binocularly to test the integrity of the visual pathway (flash VEP). Structured stimuli, such as checkerboard patterns, are also used to test the cortical response to stimuli at different

spatial frequencies (pattern VEP). Structured stimuli can be presented in either an onset / offset mode, where the stimulus is modulated between the appearance of a pattern and a blank screen, or in pattern reversal mode, when elements of the pattern are alternated (i.e. black checks become white and vice versa). Care needs to be taken with pattern stimulation to ensure that there is no overall change in luminance between the stimulus phases. Recently the multifocal paradigm has been applied to the VEP, a complex, uncorrelated visual stimulus allows the extraction of multiple VEPs representing cortical function from multiple retinal areas (Baseler et al. 1994).

There are many factors that can affect the morphology of the recorded waveforms. These include the type of stimulation (flash vs pattern onset vs pattern reversal), the size and contrast of the stimulus components as well as the speed of presentation. When the stimulus presentation rate is slow (<2 cycles per second) a complex waveform emerges consisting of multiple peaks and troughs, this is referred to as a transient response. As the rate of stimulus presentation increases the waveform becomes simpler and by 12 cycles per second it resembles a sine wave, this is referred to as a steady-state response. In addition to changes caused by the presentation of the stimulus there is considerable variability between subjects. This is both an effect of ageing and of variation within the population. In general, however, there is enough similarity between the responses from individuals to the same stimulus that conclusions can be drawn with regard to the timing (latency) of the VEP response as well as the amplitude.

Clinical Electrophysiology of Vision

Suggested minimal recording parameters for the clinical ERG (Marmor et al. 2009), mfERG (Hood et al. 2012), VEP (Odom et al. 2004; Odom et al. 2010) and EOG (Marmor et al. 2011) are published by the International Society for Clinical Electrophysiology of Vision (ISCEV). Typically visual electrophysiology recordings are represented with positive polarity toward the top of the y-axis; this is in contrast to most other electrophysiology traditions.

The normal electroretinogram

The ISCEV Standard suggests five retinal responses that test the retina under scotopic (dark adapted retina) and photopic (light adapted retina) conditions. Stimuli are presented using white light in a Ganzfeld dome to obtain even retinal illumination. The five ISCEV responses are named according to the conditions of adaptation and the stimulus luminance (flash strength in cd.s.m^{-2}). For example the dark-adapted 0.01 stimulus is a dim (0.01 cd.s.m^{-2}) flash presented to a dark adapted eye. Typical responses from a visually normal adult are shown in figure 8. The dark-adapted 0.01 stimulus (rod response) presented to a dark adapted eye is too dim to activate the cone photoreceptors, as such this response is considered as being dominated by the rod photoreceptor pathway. It consists of a slow forming wave (the b-wave) that represents the activity of the rod-bipolar cells (i.e. it is a response driven by, but not directly from the rod photoreceptors). The dark-adapted 3.0 stimulus (mixed rod-cone response) is bright enough to stimulate both rod and cone photoreceptors. The response waveform consists of an initial negative peak (the a-wave) representing photoreceptor hyperpolarisation potentially overlaid with ON-bipolar cell depolarisation and a slower positive wave (the b-wave). Superimposed on the rising edge of the b-wave are high frequency oscillations. These high frequency components can be separated from the lower frequency waveform components by using a high-pass filter that removes frequency components below about 75 Hz, these extracted oscillations are the oscillatory potentials (OPs). They represent the activity of the horizontal and amacrine cells. The light-adapted 3.0 stimulus (cone response) stimulates only the cone pathway as the rod pathway has been desensitized (bleached) by the background light. The response waveform is similar to the light adapted 3.0 response, with an a-wave, b-wave complex, but is slightly smaller and faster. Finally a light-adapted 3.0 flicker

stimulus presented at 30 Hz produces a steady-state flicker response.

For each step several trials/responses are recorded and trials with large and obvious artefacts are manually removed. The remaining responses are then averaged and the resulting waveform used for analysis. When analyzing the ERG, amplitude (normally trough to peak) and latency of the cardinal response components are measured and compared with age adjusted normal values.

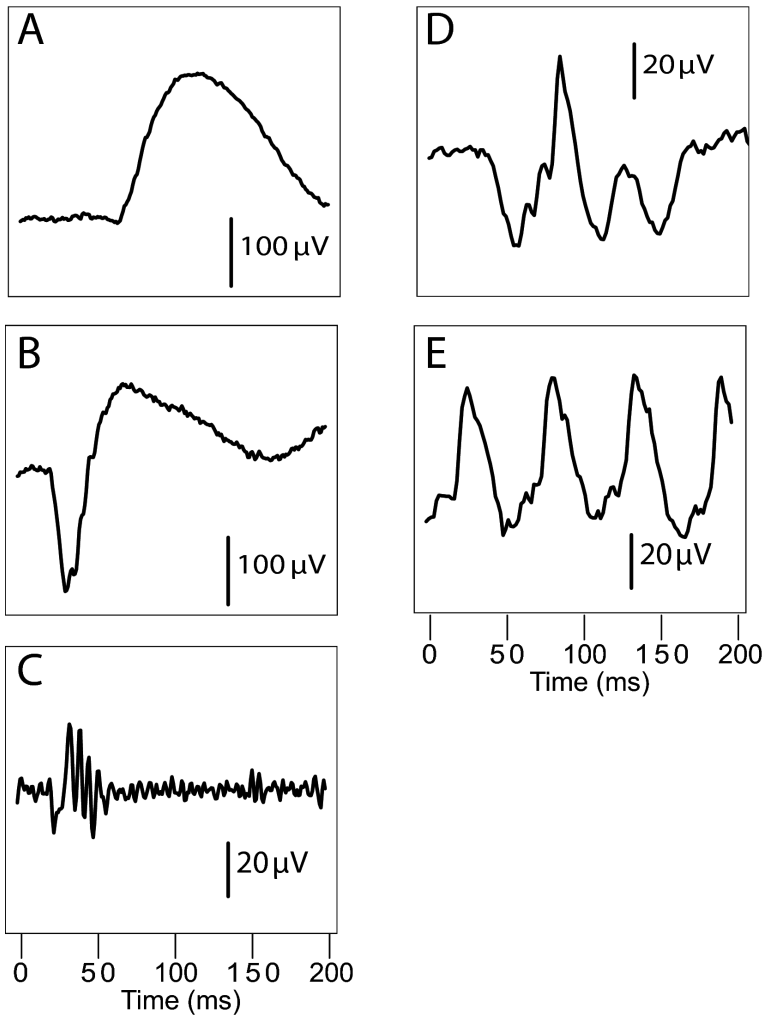


Figure 8: Electroretinogram from a visually normal adult. A) Scotopic 0.01 response, B) Scotopic 3.0 response, C) Scotopic 3.0 response filtered to extract Oscillatory Potentials, D) Photopic 3.0 response, E) Photopic 3.0 30Hz flicker response. Note the different amplitude scales in C,D and E, and different time scales in D and E.

The normal multifocal electroretinogram

The recording below (Figure 9) was recorded using a 103 hexagon stimulus array, scaled with retinal eccentricity and presented at 60Hz, mean luminance 100 cd/m²/s. The recording consists of 103 responses, each response consists of a negative, positive, negative complex, the cardinal points are named N1, P1 and N2.

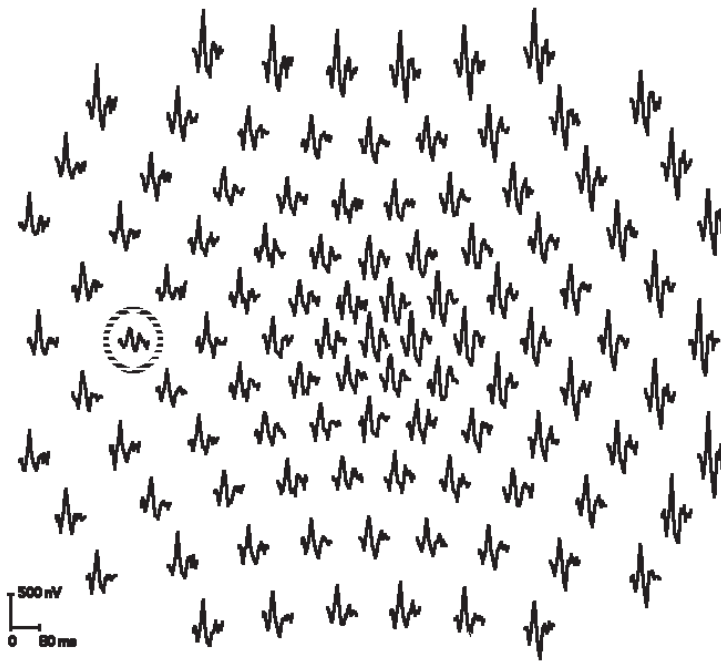


Figure 9: multifocal electroretinogram from a visually normal adult. Responses are from a left eye. The responses are shown in topographic layout, which reflects the scaling of the stimulus hexagons. Central hexagons are smaller than peripheral hexagons to compensate for the increased cone density in the central retina. The dashed circle indicates the location of the optic disc.

The normal visual evoked potential

Responses from a visually normal adult to a flash stimulus, a pattern onset stimulus and a pattern reversal stimulus are shown below (Figure 10). Pattern reversal responses are shown to a range of different check sizes.

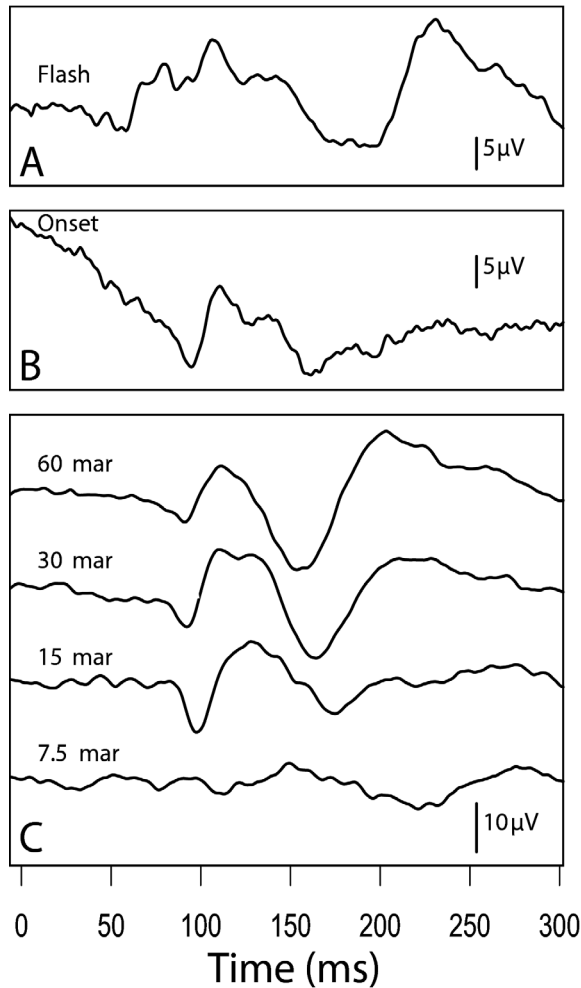


Figure 10: Visual evoked potentials from a visually normal adult. VEPs are recorded from a single electrode positioned at Oz, earlobe electrodes were used for ground and reference. A) VEP response to an unstructured flash stimulus. B) Response to 500 ms on, 500 ms off checker-board stimulus, check size was 30 minutes of arc (MAR), C) Response to a pattern-reversal checker-board stimulus, responses are shown for a range of check sizes.

Diseases of the retina

The ability of electrophysiological methods to give objective measures of visual pathway function means it has applications in the diagnosis and monitoring of many diseases. The purpose of this section is not to give a comprehensive discussion of all the diseases in which electrophysiology can give useful information, instead it is to demonstrate some of the changes that occur in electrophysiological recordings.

Rod photoreceptor dominated disease

Retinitis Pigmentosa (RP) is a large group of hereditary retinal degenerations with characteristic symptoms. The symptoms include night blindness (nyctalopia), impaired dark adaptation, progressive visual field loss (Gerth et al. 2007; Berson 1993; NIH n.d.). Abnormal pigmentation can also be observed using ophthalmoscopy which gave the disease its name (Birch 2006; Berson 1996). RP affects about 1 in 4000 people and the progression of the disease shows a large amount of variability. Mutations causing RP have been identified in at least 50 genes, about 10% of patients with RP have a mutation in the rodopsin gene (Berson 1996). Although patients may initially appear asymptomatic, reductions in the dark-adapted 0.01 ERG response have been demonstrated 10 years before the onset of symptoms (Berson 1993). As the disease progresses ERG responses become progressively more delayed in time and reduced in amplitude. At later stages of the disease the cone ERG responses may also be affected (Figure 11). The ERG is often non-recordable above noise by the third decade of patients with RP. Patients with the early stages of RP may have normal mfERGs but as the disease progresses the mfERG also shows response reductions (Dolan et al. 2002). Although in patients with advanced RP the ERG responses may be indistinguishable from noise, responses can still be identified in the mfERG (Gerth et al. 2007). The use of advanced signal detection techniques has a role in increasing the sensitivity of electrophysiological tests to aid in the early diagnosis of RP as well as to monitor remaining retinal function. This will become more important as novel therapies for RP are developed.

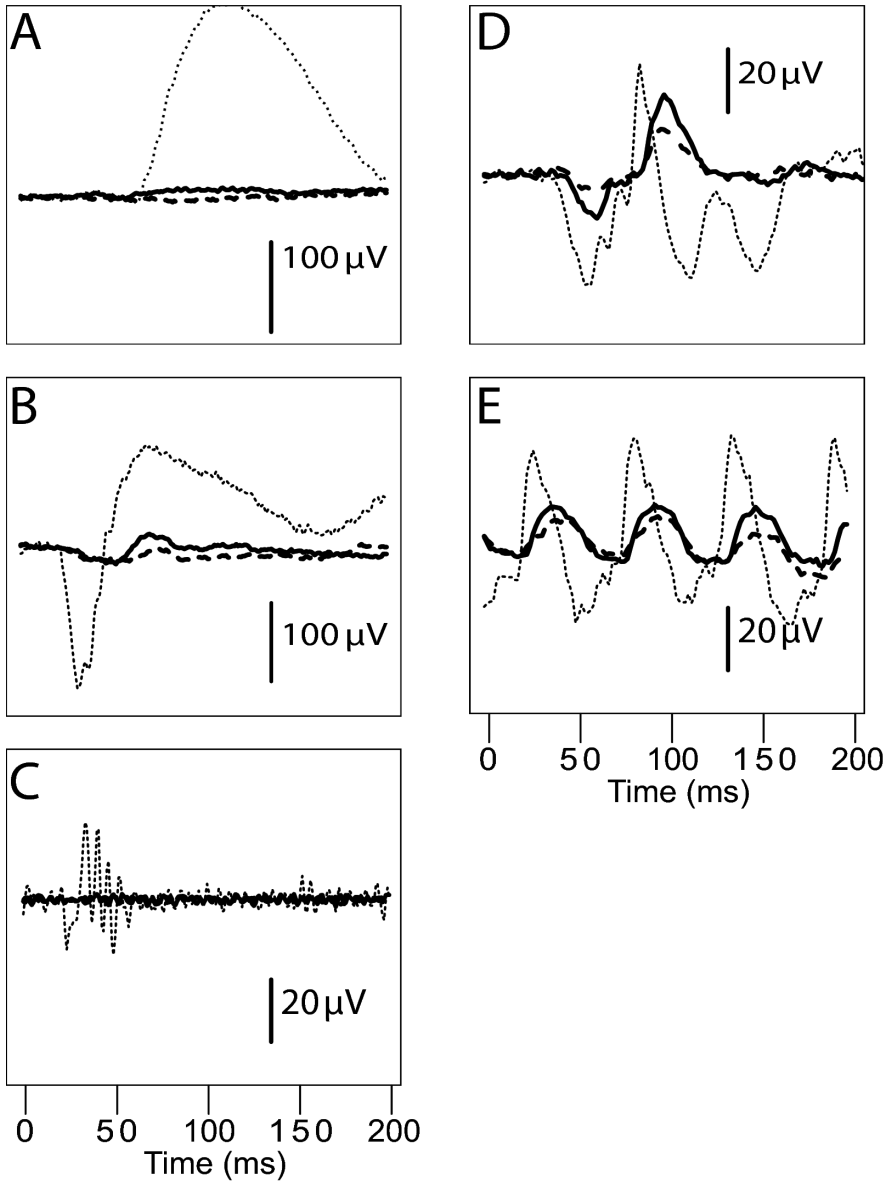


Figure 11: Electroretinogram from an adult patient with autosomal dominant RP. A) Scotopic 0.01 response, B) Scotopic 3.0 response, C) Scotopic 3.0 response filtered to extract oscillatory potentials, D) Photopic 3.0 response, E) Photopic 3.0 30Hz flicker response. Note the different amplitude scales in C, D and E, and different time scales in D and E.

Solid line = ERG performed when patient was 18 years, dashed line = same patient 5 years later. Light dotted line = healthy adult.

Cone photoreceptor dominated disease

Stargardt Macular Dystrophy (STGD) is a hereditary disease characterized by a progressive loss of central visual acuity. The onset of symptoms varies considerably with 60% of patients presenting with impaired vision in the first two decades of life and 20% not experiencing decreased vision until the fifth decade.

STGD is caused by mutations in the ABCA4 gene. This gene codes for an ATP binding protein (ABCR) found in the membranes of photoreceptor outer segments. ABCR is normally involved in the recycling of retinol, one of the key proteins involved in photo-transduction. Defective ABCR protein leads to a build-up of a protein N-retinylidene-PE (N-RPE) in the outer segment of the photoreceptor. Normally the photoreceptor outer segments are ingested by the retinal pigment epithelium (RPE), however a bi-product of N-RPE, N-retinylidene-N-reinl-PE (A2E), accumulates as indigestible lipofuscin (Lodha 2007; Jung et al. 2007). In vivo measurements of lipofuscin in patients with STGD demonstrate that the amount of lipofuscin is 2-5 times greater than in age-matched control subjects (Delori et al. 1995). Eventually the build up of lipofuscin proves toxic to the RPE cells and photoreceptor cells die secondary to loss of RPE support. The density of photoreceptors is greatest in the central retina (fovea and macular), leading to the greatest rate of accumulation of lipofuscin and subsequent cell death occurring in this region.

The electroretinogram is a test of global retinal function, it is estimated that at least 20-30% of the retina needs to be affected before significant changes are observable in ERG recordings. As a result, in the early stages of STGD the ERG often appears normal. Because the mfERG is able to measure retinal function from much smaller areas of retina, abnormalities are often detected much earlier with the mfERG compared with the ERG (Figure 12).

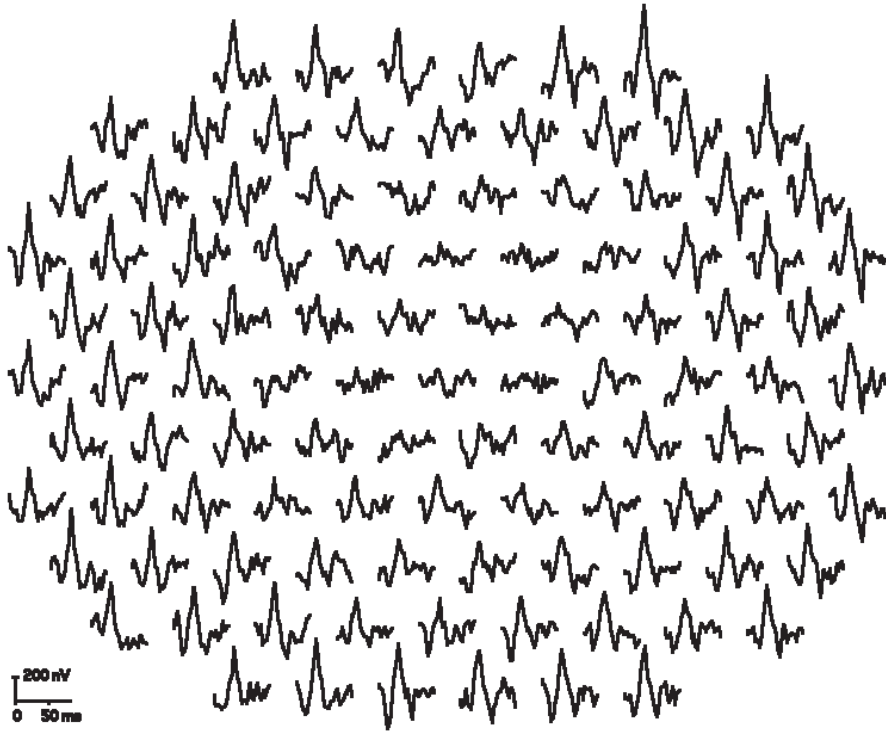


Figure 12: Multifocal electroretinogram of patient with Stargardt Macular Dystrophy. Recording is from the patient's right eye and shows reduced cone responses in the central 5-10°.

As with RP, techniques that increase the sensitivity to changes in the mfERG will enable the monitoring of the progression of STGD.

Middle retina disease: X-linked Congenital Stationary Night Blindness

Congenital Stationary Night Blindness (CSNB) is a heterogenous family of hereditary disorders with similar phenotypes. The characteristic phenotype is abnormal night vision (nyctalopia) from birth. The phenotype also typically includes variable levels of reduced visual acuity, myopia, strabismus and nystagmus (involuntary eye movements). Different forms of CSNB have been shown to have X-linked, autosomal dominant and autosomal recessive inheritance patterns (Audo et al. 2008; Miyake 2006). The X-linked inheritance

mode is associated with two forms of CSNB, CSNB1 (complete x-linked CSNB) and CSNB2 (incomplete x-linked CSNB). Initially the two forms were distinguished based on electrophysiology and psychophysical testing (Miyake et al. 1986). More recently they have been confirmed as distinct diseases with the identification of two separate mutations (Bech-Hansen et al. 1998; Bech-Hansen et al. 2000).

CSNB1 is caused by mutations in the NYX gene that encodes the protein nyctalopin. The nyctalopin protein is thought to play a role in the formation of synapses with the rod-bipolar and cone ON-bipolar cells (Bech-Hansen et al. 2000). CSNB2 is caused by mutations in the CACNA1F gene, this gene is thought to have a role in regulating the release of glutamate from the photoreceptor (Bech-Hansen et al. 1998; Mansergh et al. 2005).

Both CSNB1 and CSNB2 show a typical, abnormal response to a 3 cd scotopic stimulus, referred to as a Schubert-Bornschein, or electronegative response (Schubert & Bornschein 1952). The response shows a normal (often supernormal) a-wave with a markedly reduced b-wave. The 0.01 cd scotopic flash (rod response) is indistinguishable from noise in CSNB1 while in CSNB2 it is reduced but still measurable. Responses to a 3 cd photopic flash (cone response) are relatively normal with CSNB1, although the a-wave shows a characteristic flattening of the a-wave trough. Cone responses from patients with CSNB2 are very attenuated, similarly the responses to the 3 cd 30Hz flicker responses are normal in CSNB1 and significantly reduced in CSNB2 (Figure 13). The use of a long duration (200 ms) flash stimulus allows separation of the ON and OFF responses in the ERG. The response to flash onset is not observable in CSNB1 while the response to flash offset is. As expected neither response is detectable above noise in CSNB2.

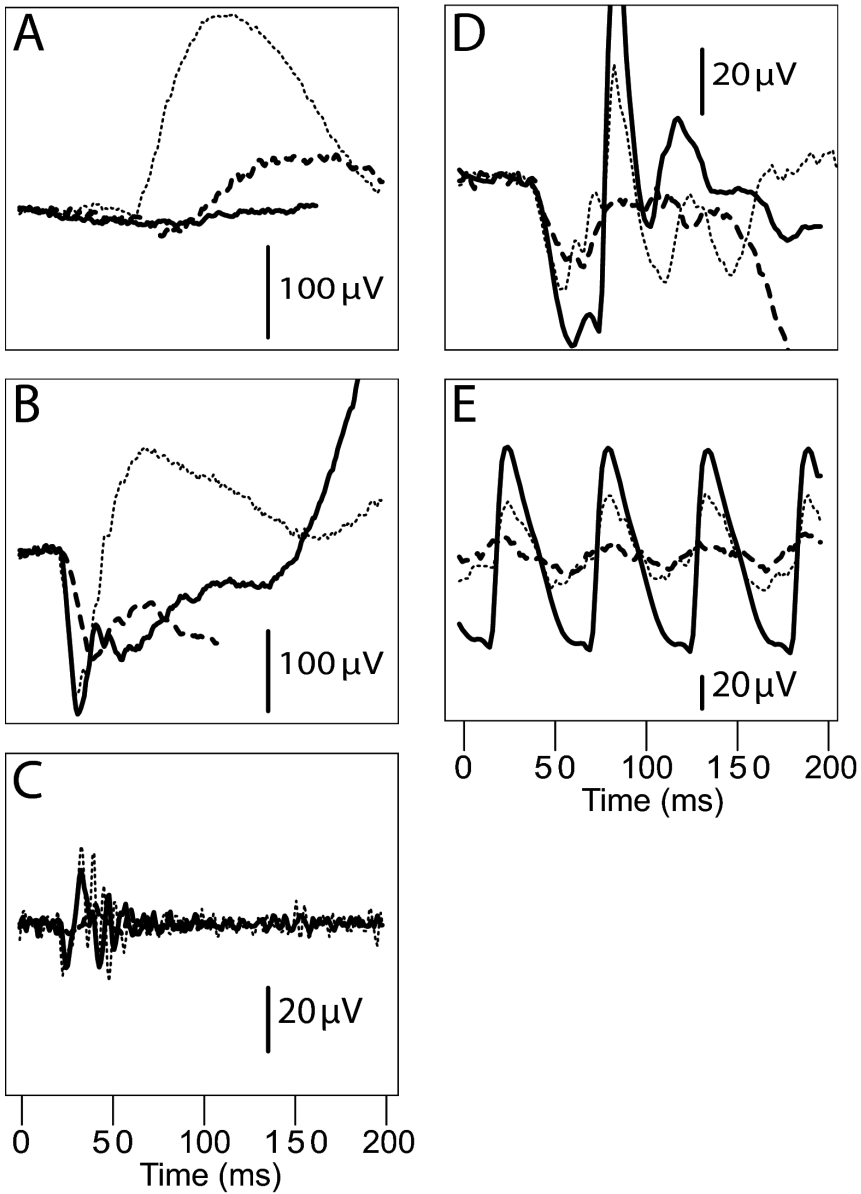


Figure 13: Electretinogram from patients with Congenital Stationary Night Blindness. A) Scotopic 0.01 response, B) Scotopic 3.0 response, C) Scotopic 3.0 response filtered to extract oscillatory potentials, D) Photopic 3.0 response, E) Photopic 3.0 30Hz flicker response. Note the different amplitude scales in C, D and E, and different time scales in D and E.

Solid line = Type I (complete) CSNB, dashed line = Type II (incomplete) CSNB, Light dotted line = healthy adult.

The mfERG is not usually performed on patients with CSNB as there is little clinical value. However it has been shown, however, that the first order mfERG responses are delayed globally across the retina with normal amplitudes in patients with CSNB1. It is suggested that the delays represent abnormalities observed in the 2nd order mfERG kernels that represent the adaptation of the retina to repeated flashes (Kondo et al. 2001).

While the electrophysiological features of patients with CSNB are clear, the results may be complicated by the patient's inability to comply with the testing procedure. For example the associated nystagmus or a patient's young age can greatly increase the noise in the recording making identification of the waveform changes harder to discern.

Diseases affecting the cerebral visual system

Ocular Albinism

Albinism is a group of diseases caused by mutations in genes that control the production of melanin or the formation of melanosomes (intracellular vesicles that manufacture and hold melanin). Melanin is a pigmented protein involved in skin colour, hair colour and tanning (Levin & Stroh 2011). In addition melanin is found in the iris, choroid and retinal pigment epithelium of the eye. The typical phenotype of people with albinism is often thought to be complete hypopigmentation leading to light skin, white hair and pink-eyes. Often however mutations causing albinism are phenotypically normal, with dark skin and brown or black hair. In contrast some ethnic groups (e.g. those from Scandinavia) naturally appear very lightly pigmented. The determination if albinism is present depends on the presence of ocular abnormalities (Levin & Stroh 2011). A reduction in the amount of pigmentation in the RPE causes several problems in the development of the eye and visual pathway. Macular (or foveal) hypoplasia is pathognomonic for albinism, blood vessels can be observed in the normally avascular macular zone and the foveal pit is shallow or absent. This often leads to reduced visual acuity and nystagmus. When albinism occurs in conjunction with hypo-pigmentation of the skin it is referred to as oculocutaneous albinism (OCA), when only ocular phenotype is present it is referred to as ocular albinism (OA). Albinism is also related to abnormal neurogenesis of the optic pathway. It is unclear if this is a direct result of the

reduction of melanin or if it related to other factors involved in the melanin pathway (Mason & Erskine 2004). In the presence of melanin retinal ganglion cells from the nasal hemisphere of the eye (proximately 50% of the total) cross at the optic chiasm before passing to the LGN in the contra-lateral cortex. Fibres from the temporal retina project to the LGN in the ipsilateral hemisphere (Figure 14). When the eye develops in the absence of melanin an increased proportion of fibres cross at the optic chiasm. Despite this misrouting of fibres from the temporal visual fields visual field testing can be normal demonstrating the remarkable plasticity of the visual system in patients with albinism (Apkarian & Bour 2006).

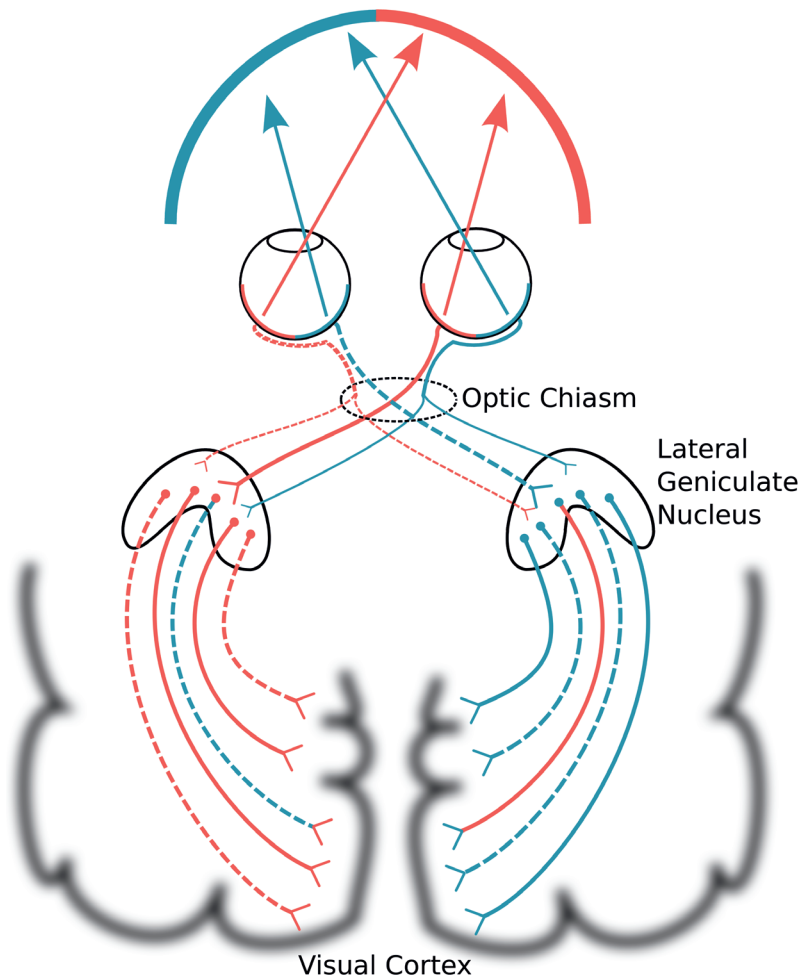


Figure 14: Schematic diagram showing chiasmal misrouting in Ocular Albinism.

Although the ERG of patients with albinism is often difficult to record due to eye movements, it is usually normal or super-normal. This increase in amplitudes is caused by the increased scattering of light caused by the hypopigmented RPE. The chiasmal misrouting can be measured using a multichannel VEP. The VEPs recorded, in response to monocular stimulation, from electrodes placed over each hemisphere of the visual cortex (rather than over the mid-line) demonstrate contra-lateral hemispheric response lateralization. That is to say the response recorded from the left cortex is larger in amplitude and earlier in timing than that from the right cortex when the right eye is stimulated. The reverse is true for left eye stimulation. The detection of the response lateralization is complicated both by the high variability of VEP amplitudes and by the developmental changes to VEP morphology that occur during the first years of life. Several methods have been proposed for detecting this lateralization, these include the asymmetry index where amplitude at each electrode location is measured (as area under the curve) and amplitudes from left and right eye stimulation compared (Apkarian et al. 1983). Soong et. al. recommended calculating an inter-hemispheric difference potential by subtracting the response recorded from the left hemisphere from that recorded from the right hemisphere. Pearson's measure of correlation is then used to quantify the amount of lateralization (Figure 15). This method was shown to have a sensitivity of 86% with specificity of 81%. The imperfect sensitivity value was ascribed to variations in the amount of misrouting, while the imperfect specificity may have been due to difficulties in testing children or to the presence of undiagnosed carriers of an albinism gene (Soong et al. 2000).

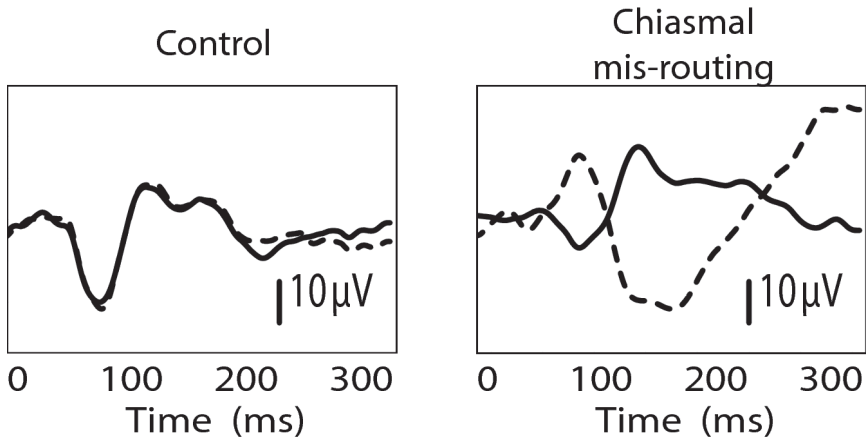


Figure 15: Visual evoked potentials demonstrating chiasmal misrouting. Waveforms are inter-hemispheric difference potentials ($O_2 - O_1$). Solid lines = Right eye stimulation, dashed lines = Left eye stimulation.

The reduction of information involved in using a single calculated number to determine the degree of lateralization can be problematic. A correlation measure can be calculated on any two waveforms and gives no indication of the magnitude of the responses. Thus it is possible that misleading results could be obtained in situations in which recordings are noisy, or the response is reduced. Whenever this type of data reduction analysis is performed, care must be taken to consider other metrics of waveform quality.

Assessing Visual Acuity with the visual evoked potential

Clinical measurement of visual acuity often uses psychophysical techniques, these include reading letters or identifying symbols of progressively decreasing size or Preferential Looking tasks. Many patients lack the necessary abilities to comply with these forms of testing due to immaturity, learning difficulties, motor and intellectual impairment (Mackay et al. 2008). The VEP is an objective testing method that has been used with a high success rate in populations with neurological and developmental delay (Skarf & Panton 1987). Relatively early it was determined that VEP amplitude was dependent on both the stimulus size and visual acuity (Harter & White 1970). Transient VEPs are recorded to a series of varying spatial frequencies and visual acuity is reported

as the highest spatial frequency where a repeatable response can be recorded (figure 10). The accurate recording of VEPs depends on many factors not least of which is the behavioural state. Inattention can lead to unreliable recordings. Recently a more rigorous approach to threshold determination for transient VEPs was proposed using a successive approximation algorithm (Mackay et al. 2008), this technique was able to reduce recording times significantly. The sweep VEP method has also been used to reduce recording times and thus reduce the problem of patient inattention. Here a steady-state VEP response is recorded to a fast reversing stimulus, the stimulus can be quickly swept through a range of spatial frequencies. It has been shown that this technique can reduce the recording time to a period of several (10-20) seconds (Almoqbel et al. 2008).

Although VEP estimates of visual acuity have been shown to correlate with other psychophysical measures, estimates of visual acuity have been found to differ by up to 132 fold, with the amount of difference being inversely proportional to the visual acuity (Mackie et al. 1995). This may reflect differences in what is being measured. The VEP is testing the visual pathway up to the primary visual cortex, while behavioural measures are also testing higher cortical processing. Many neurological disorders, such as nystagmus and seizure disorders, increase the background 'noise' of the VEP, making accurate detection of the VEP more difficult (Hoyt 1984). Signal detection algorithms are able to improve the speed and quality of transient VEP recordings. The ability to identify smaller VEP responses, such as those produced by higher spatial frequency stimuli, will improve the accuracy of visual acuity estimates.

Optic Neuritis

Optic Neuritis (ON) is the term given to a demyelinating neuropathy affecting the optic nerve. The neuropathy can be present either on its own or in association with other infectious or inflammatory diseases such as Lupus or Multiple Sclerosis (Pau et al. 2011). Typical symptoms of ON include a sudden loss of vision (usually monocular), a loss of colour vision, changes in the pupillary reactions to light and pain on moving the eye (Zieve & Lusby 2011). Often the symptoms are temporary and vision will return to normal within 2-3 weeks. The cause of ON is presumed to be an inflammatory process leading to neuronal cell death and axonal degeneration. The pattern-reversal VEP is the

current test of choice for confirming clinical and subclinical ON. The P100 component shows a significant delay in 60-80% of cases after an episode of ON (Frederiksen & Petrera 1999; Naismith et al. 2009). Since the VEP is dominated by the macular response it has been suggested that the multifocal VEP may increase this sensitivity by allowing responses from more peripheral retinal areas to be extracted (Klistorner et al. 2008).

Summary

The effects of disease on the retina and visual pathways can be observed by electrophysiological methods. Careful modification of stimulus, recording and analysis parameters can help elucidate where a lesion is located. Changes to the ERG and mfERG can manifest as reductions in amplitude and / or delays in timing. Changes may affect the complete response or just individual components. It is worth noting that changes to an early element of the visual pathway will often be reflected in later elements. For example a reduced a-wave caused by loss of photoreceptors will often lead to a reduced b-wave, although the underlying disease does not affect the middle retinal cells. Amplitude changes in the ERG are often thought to represent a reduction in the number of functioning cells, while delays in response timing are often thought to represent reduced sensitivity in phototransduction and inter-cell signalling.

VEP latency changes, normally representing demyelination of the optic nerve, are usually the most important finding. VEP amplitudes are highly variable between individuals and as a result quantitative analysis of amplitudes is rarely used. Comparisons of amplitude can be made within the same subject, as when using the VEP to test visual acuity, or in special cases when optic pathway changes are studied.

All electrophysiological responses undergo developmental changes, in the case of the VEP these changes can last well into adolescence (Dustman et al. 1977). There is also evidence that VEP responses have shorter latencies in females, it has been suggested that this is related to head size (Emmerson-Hanover et al. 1994; Gregori et al. 2006; Malcolm et al. 2007). The ERG reaches adult values around 5 years of age (Westall et al. 1999). In later life the development of opacities in the optic media can also have an effect on the recorded responses.

As such the age of the subject needs to be considered when interpreting results. Finally electrophysiological recordings are very sensitive to the behaviour of the patient, and any difficulties with compliance also need to be considered in the interpretation.

The application of signal identification techniques and the use of objective measures of signal quality will probably improve the accuracy of clinical visual electrophysiology testing. Advanced multivariate analysis methods, which consider the total recorded waveform instead of requiring data reduction, may be able to identify novel features that reveal more information about the disease process or aid in diagnosis.

Signal Analysis

Many of the problems involved in recording electrophysiological evoked potentials are common to all testing modalities. The primary problem reducing of the massive amount of recorded data into an amount that allows practical conclusions to be drawn. To do this the data must be sifted to separate the components of interest (the signal) from everything else (the noise). As has been pointed out elsewhere this sifting process risks excluding or ignoring potentially useful information (Regan 1989).

Typically the potentials of interest have relatively small amplitudes which require them to be amplified before they can be recorded, often amplification factors of 10^4 to 10^5 are used. While some effort can be made to exclude potentials from this amplification based on their frequency much of the background noise falls within the same frequency bands as the signal of interest so cannot be excluded. While this problem is less pronounced for electroretinographic recordings, VEPs typically have 100x less power (10x less amplitude) than the background noise. As noise is defined as any changes to the recorded electrical potential that are not related to the visual stimulus it can come from a variety of sources. These can include unrelated brain activity, electrical potentials generated by muscle contractions as well as external sources of noise such as electrical mains current oscillations.

Signal analysis can be grouped into 3 areas, artifact rejection, averaging and component selection. Typically the analysis performed in most clinical (and many research) visual electrophysiological recordings is relatively basic.

Artifact rejection can be performed in real-time, as the responses are recorded, or post-hoc. Real-time artifact rejection is performed by filtering the incoming signal to isolate only the frequency bands of interest. Threshold rejection algorithms are often used, these identify responses thought to contain electrical potentials that are too large to be generated by the physiological process of interest. Typically the threshold rejection algorithms are relatively simple, for example all responses with potentials $> \pm 100 \mu\text{V}$ may be rejected. Post-hoc

rejection usually involves a human examining the recorded waveforms and manually excluding responses. In addition to being a time-consuming process, this subjective analysis is open to observer bias.

When averaging is performed it is typically a basic algorithm in which all the responses remaining after the artifact rejection step are given equal weighting in the final average.

Component selection is probably the most important part of the analysis. Normally the waveform to be analysed consists of one or more features (troughs and / or peaks) that are conserved across subjects. These features are identified either by simple algorithms (minimum/maximum amplitude within a specified time window) or by human experts (peak picking). The timing and amplitude of these cardinal features are then used in the interpretation of the waveform. This peak picking process has many disadvantages. Often the troughs and peaks formed by different physiological processes overlap each other or are contaminated with noise potentials making identification of the true peak ambiguous. The reduction of the waveform to a few cardinal features of necessity means a lot of potentially valuable, information is disregarded.

The current situation in the clinical visual electrophysiology domain, where complex waveforms are often reduced to a few cardinal features, identified by observers with a range of experience, is obviously susceptible to subjective interpretation. The naive analysis of poor quality waveforms can often lead to inaccurate and misleading results. The data reduction involved potentially excludes important information that can aid in the interpretation of the electrophysiological signal. These problems are common to many fields requiring the analysis of electrophysiological signals including visual electrophysiology, electroencephalography (EEG), electromyography (EMG) functional magnetic resonance imaging (fMRI), electrocardiography (ECG) and others. Techniques have been developed that improve the quality and sensitivity of recordings by improving signal detection e.g. (Cuypers & Thijssen 1995; Harris & Woody 1969; Ihrke et al. 2009; Lange et al. 2000; Vincent 1992; Zhang & Hood 2004), reduce subjectivity by introducing metrics of signal quality e.g. (Simpson et al. 2009; Meigen & Bach 1999; Victor & Mast 1991;

Young & Kimura 2010; Zhang et al. 2002) and ameliorate the effects of data reduction (Fisher et al. 2007; Haig et al. 1995; Hood & Li 1997; McIntosh et al. 1996; Najafabadi et al. 2006; Masic & Pfurtscheller 1993; Zhou et al. 2007).

The application of new signal identification and analysis techniques promises to greatly enhance the applicability of visual electrophysiology. Before any new analysis techniques can be applied it is important to characterise their performance. Often this characterization is expressed in terms of sensitivity and specificity. Accurate calculation of sensitivity and specificity relies on knowing the underlying truth (a gold-standard), e.g. presence or absence of disease. In the medical field this information is often not as clear cut, for example a particular disease may have differential effects on electrophysiological responses in different patients or over time. While it is possible to characterise the new technique in terms of another established technique this is an imperfect solution. An alternative is the artificial simulation of diseases on otherwise well characterised recordings. Care needs to be taken that the simulation techniques used are in fact representative of the changes observed in real life.

Signal extraction in the frequency domain

The primary tool for the analysis of waveforms in the frequency domain is Fourier decomposition. The Fourier Theorem demonstrates that any waveform can be broken down into a series of sine waves of appropriate phase and frequency. This means that any waveform can be represented as a series of frequencies with different power. Any waveform can be either periodic (repeating in time from $-\infty$ to $+\infty$) or aperiodic. Since the Fourier decomposition of an aperiodic waveform requires an infinite number of sine waves it is not practical to perform a Fourier analysis on an aperiodic wave. As it is not possible to sample any wave stretching to infinity this limitation is usually overcome by imagining the sample as repeating.

As has been discussed already regarding VEPs, as the frequency of the stimulus increases the complexity of the recorded waveform decreases eventually approximating a sinusoidal wave. The same holds true of retinal evoked potentials. The power spectrum of the steady-state waveform shows that the power is concentrated in very narrow frequency bands based around the primary

frequency of the stimulus and its harmonics. This transfer from the transient response to a steady-state response has many advantages for signal analysis. Since, by definition, noise is any recorded response not related to the stimulus it becomes possible to analyse only waveform components that fall into frequency bands that are harmonics of the stimulus. Unfortunately a draw-back of steady-state responses is that much of the underlying physiological complexity is lost. As a result most clinical visual electrophysiology relies on the more complex transient waveforms. As most transient waveforms contain both slow and fast components their power is spread out over a much greater range of frequencies. Power spectral analysis of VEP waveforms generated by a moderately fast 4 Hz stimulus indicated that they contained power in frequencies up to around 50 Hz (Trick et al. 1984) and it has been demonstrated that ERG recordings contain significant power at frequencies > 100 Hz (Lachapelle & Benoit 1994). Because many of the potentials that contribute to the noise in an electrophysiological recording fall within the same frequency band as the signals of interest, excluding noise is difficult by using frequency based filtering.

A major disadvantage of studying electrophysiological potentials in the frequency domain is the loss of any information about the timing of any of the frequency components. Information about the exact timing of the components forming the recorded waveform is often useful in determining the underlying physiological processes.

Another method for decomposing an arbitrary waveform into its constituent frequencies is the wavelet transform. A wavelet is a wave-like oscillation with an amplitude that starts at 0 and oscillates at a specific frequency and ends after a specific time at 0. The wavelet transform compares the recorded waveform with a series of different wavelets with different frequencies. By sliding the wavelets along the recorded waveform it is possible to build a map of how much a particular frequency contributes to the waveform at a particular time. While wavelet analysis has been applied to visual electrophysiological signals (Thie et al. 2012) it is limited by the relationship between time and frequency. As the frequency of the wavelets decreases, the accuracy with which they can be located in time also decreases. This makes wavelet analysis for the slower waveform components particularly insensitive to changes in time.

Signal extraction in the time domain

An early attempt to separate the signal from the noise was the superimposition technique (Dawson 1947). This involved triggering the sweep of an oscilloscope synchronously with the onset of the stimulus. The displays of the oscilloscope from multiple trials were then superimposed on the same photographic plate. Features of the response occurring at a constant time after stimulus onset become more clearly defined on the photographic plate after a number of sweeps. While this technique does not lend itself to the precise quantitative measurement of the evoked potential it has the advantage of giving a direct visual indication of the variability between trials (Regan 1989).

The superimposition technique is basically an additive process; waveform components occurring at the same time after the stimulus are 'added' together. A development of this process is signal averaging. In signal averaging recorded trials are summed together then divided by the number of trials. The main advantage of this over superimposition techniques is that waveform components that do not consistently occur at the same time after the stimulus are reduced. While signal averaging is often a successful technique in practise there are some underlying assumptions that have been questioned.

1. The recorded waveform is the sum of two independent waveforms, the signal waveform and the noise waveform.
2. The signal waveform is stationary (i.e. stays the same over multiple trials).
3. The noise waveform is random with a mean amplitude of 0.

If these conditions hold true, signal averaging can be shown to be the most efficient method for improving the SNR giving a reduction in noise of \sqrt{N} , where N is the number of trials. Unfortunately all these assumptions have been called into doubt. It is unclear if the principle of independence between the visually evoked signal and other brain activity is true. Some researchers have found that the alpha waves in the brain can be modulated by a visual stimulus e.g. (Arieli et al. 1996), other research has found no effect e.g. (Risner et al. 2009). The stationarity of the signal waveform has also been called into question. In a study of individual trial responses to a flash stimulus Möcks and Gasser found that 11.5% of participants had significant amounts of variation in

trial amplitude, 29.5% showed a significant change in latency over the duration of the recording session (drift) and 28.2% showed significant change of latency between trials (jitter) (Möcks et al. 1987). Finally, because the size of electrical potentials generated by muscle artifacts are much greater than those from cortical activity it is easy for average of the noise to move from 0 amplitude.

Many methods have been used to address these limitations. Both manual and automatic algorithms have been used to eliminate trials that are contaminated by large artifacts such as muscle potentials. An adaptive averaging algorithm was proposed in 1967 to address the effect of latency shifts between trials. This algorithm worked by shifting the individual trials in time so as to maximize the correlation between the trials (Woody 1967).

Other component extraction methods, such as principle component analysis, (PCA) and independent component analysis (ICA) have been applied to electrophysiological recordings (Zhang & Hood 2004; Vincent 1992; Knuth et al. 2006; Ihrke et al. 2009; Velde 2000). Both these algorithms are examples of blind source separation. The underlying assumption is that the recorded signal is a linear mix of signals from a set of independent sources. If the underlying sources are sampled from different locations (e.g. different electrodes) the underlying sources contribute differently to the recorded signal. PCA attempts to estimate the different sources by minimising the correlation between them, while ICA attempts to estimate the sources by making the estimated sources as non-Gaussian as possible. A key requirement for both PCA and ICA is that the number of sources be equal to or less than the number of samples. This precludes their use on ERG recordings which are normally recorded from a single channel. VEP recordings, however, are performed often using more than one electrode, making VEPs a potential candidate for these techniques. The multifocal techniques can also be considered as recording information from multiple channels, although in this case the multiple channels are the input rather than the output, and PCA has been successfully applied to extract signals from multifocal visual evoked potentials (Zhang & Hood 2004). A disadvantage of source separation methods, such as PCA and ICA, is the identified components can rarely be directly linked to underlying physiological processes and the selection of components for further analysis is largely subjective (James & Hesse 2005).

The signal averaging methods described above have the advantage of assuming no prior knowledge about the morphology of the waveform. Often previous knowledge about the waveform is unavailable, if for example there is too much variation between subjects or if the disease process is unknown. In other situations however the morphology of the waveform is relatively constant. Several algorithms have been suggested that use this prior knowledge. A recent development is the use of expert systems such as neural networks for signal identification. These systems are trained to recognise a known underlying waveform from data that has been contaminated with noise. These systems have been shown to be successful in signal identification (Simpson et al. 2009).

Analyzing waveforms in the time domain

Once the underlying waveform has been suitably estimated there is still the requirement to reduce it to a form suitable for comparison. Often this is done by identifying typical peaks and troughs, which are highly conserved across multiple subjects and recording the timing and / or amplitude of these. While this method is very successful when the features are clearly defined, slow frequency components may not form clear peaks or troughs. Since the analysis is based on the location of a single time point, often relatively small amounts of noise can obscure the exact location of the feature. If multiple features are superimposed on each other, the peaks and troughs can be obscured.

A technique that has shown considerable applicability to the analysis of mfERG data is template based analysis (Hood & Li 1997). This technique uses a well characterised template waveform that is modified (e.g. stretched in time, or amplitude) to match the recorded waveform. This technique has the advantage that the complete recorded waveform can be considered in the analysis, however the description of changes to the recorded waveform are limited to the modifications chosen by the experimenter.

Partial least-squares (PLS) analysis is similar to PCA analysis in that the variation in the analysed data is partitioned into different sources, however, in the case of PLS analysis the solutions are constrained to those attributable to experimental manipulation (Friston et al. 1993; Moeller et al. 1987; Krishnan et al. 2011). PLS analysis has been used to identify patterns of brain activity related to behavioural responses and other experimental stimulation as well as between individual brain regions and the rest of the brain. PLS analysis has been adapted for use on spatial-temporal data such as event evoked response

potentials (ERPs) (st-PLS) (Itier et al. 2004; McIntosh & Lobaugh 2004). In this context st-PLS identifies the specific combination of waveform differences that distinguish experimental conditions. A key advantage of st-PLS is that it can provide a statistically rigorous analysis of waveform differences without requiring the compression of the spatial or temporal information in the data. We have applied st-PLS to identify patterns of change to retinal responses that occur in patients with Type 1 Diabetes.

Measuring signal quality

A problem closely related to signal extraction is measuring the quality of the extracted signal. If the recorded waveform is considered a mixture of a signal waveform and unrelated noise then a key measure of quality is the ratio of the SNR in the extracted waveform. Key to accurate calculation of the SNR is obtaining an accurate measurement of the noise. When recordings are analysed in the frequency domain it is often assumed that signal components must exist in frequencies that are harmonics of the stimulus frequency, thus noise can be accurately estimated using power from frequencies that are not harmonics of the stimulus. In the time domain noise is often taken as the recorded waveform in the absence of a stimulus. Unfortunately there is considerable evidence that the brain responds differently when a stimulus is not present, for example occipital alpha activity increases when the eyes are closed. An alternative is to separate the recorded waveform into an epoch containing the signal and another epoch separated in time which is not affected by the signal potentials (the noise epoch); often an epoch before stimulus onset is chosen for this. Care needs to be taken with this approach that no slow potentials influence the noise epoch. A better estimate for noise is provided by the plus-minus method, where multiple trials are alternately added and subtracted to form a resultant waveform in which any repeating components are cancelled out (Schimmel 1967).

When multiple trials to the same stimulus are recorded it is possible to test the consistency of the recorded waveform. In the frequency domain the circular T statistic is used to test the consistency of the phase and power of the response at a particular frequency (Victor & Mast 1991). Recently a technique has been published for testing if a single waveform is significantly different from noise. This technique works by using a noise sample as a template to simulate multiple different estimates of the potential noise (Young & Kimura 2010), the peak

amplitude of the recorded waveform is then tested to see if it is greater than the maximum amplitudes of the estimated noise.

Objectives

To investigate objective methods of identifying changes in visual electrophysiological recordings.

Can objective methods be used to detect electrophysiological signals?

What metrics can be used to quantify the performance of different signal detection methods?

Specific objectives and aims

Paper I

To optimise an objective method for detecting multifocal electroretinogram responses that have been reduced due to disease.

Aim 1: Simulate the effects of disease by artificial modification of healthy mfERG recordings.

Aim 2: Measure the performance of 3 automated signal detection algorithms and compare performance to that of expert human observers.

Paper II

To develop real-time signal detection methods that can be used to improve the quality, and reduce the recording time of the pattern-reversal visual evoked potential.

Aim 1: Develop objective measures of signal quality.

Aim 2: Compare the performance of 4 different signal identification algorithms.

Paper III

To demonstrate a novel application of a multivariate analysis technique, spatio-temporal partial least squares analysis.

To elucidate changes to retinal function that occur with Type 1 Diabetes before the onset of clinical retinopathy.

Methods

Recording protocols

Multifocal Electretinogram (mfERG) Paper I & III

Recordings were recorded monocularly on an eye chosen randomly. The subject's pupil was dilated using topical application of 1% tropicamide and 2.5% phenylephrine hydrochloride. Standard mfERG's were recorded using the Veris™ system (Electro-Diagnostic Imaging, Redwood City, CA, USA). The stimulus consisted of 103 hexagons controlled using an m-sequence of length $2^{15}-1$, the stimulus rate was 75 Hz for paper I (~7 minutes recording time) and for paper III 60 Hz (~9 minutes recording time). Mean stimulus luminance was 100 cd.s.m². The stimulus was presented using the FMS II Stimulator, this unit contains a through-pupil fundus camera operating in the infra-red, which allows simultaneous monitoring of fixation. The recording sessions were split into 16 segments and any segments with excessive fixation loss, or increased noise were repeated. Bipolar Burian-Allen contact lens electrodes (Hansen Laboratories, Coralville, IA, USA) were used with a gold-cup Grass electrode (Grass Technologies, West Warwick, RI, USA) placed on the forehead for the ground electrode. Analog bandpass filtering (10-300 Hz) was applied using a Grass Telefactor TCP511 A.C. Amplifier (Grass Technologies, West Warwick, RI, USA) and the signal was amplified 50,000x.

The subjects in paper III undertook a second multifocal protocol, the slow flash multifocal electroretinogram (sf-mfERG). In this protocol the stimulus was slowed by inserting 5 frames in which all the hexagons were dark after each multifocal stimulus frame. The inserted blank frames slowed the stimulus rate to 10 Hz, allowing a more complex response waveform to develop. An additional 75 Hz digital filter was applied to these recordings, allowing the extraction of high frequency oscillatory components thought to represent the function of inner retinal components (Kurtenbach et al. 2000). This protocol always followed the standard mfERG protocol.

Visual Evoked Potentials (VEP) Paper II

VEPs were recorded using Neuroscan Acquire (Compumedics Neuroscan, Charlotte, NC, USA) system. Stimuli were generated using VisionWorks™ StimulusMaker™ software (Vision Research Graphics, Durham, NH, USA) and presented on a CRT monitor. The monitor subtended approximately 20° of the visual field. The stimulus consisted of a black and white checker-board pattern (mean luminance 80 cd.s.m², Michelson contrast 80%) presented in pattern-reversal mode at 0.5 Hz (2 reversals per second). Each black and white check filled approximately 15 minutes of arc (MAR). Three gold cup electrodes (Grass Technologies, West Warwick, RI, USA) were placed over the occipital cortex (positions O1, Oz and O2 of the International 10-20 System (Klem et al. 1999)). Ground and reference electrodes were placed on the earlobes. Only the Oz channel was used in the analysis.

Signals were recorded in continuous mode and a 1-300 Hz bandpass digital filter was applied using the Acquire software. An artefact rejection algorithm was used to exclude trials with potentials $\geq \pm 100 \mu\text{V}$. The recorded waveforms were further filtered using a 1-40 Hz bandpass digital filter and then split into 500 ms. epochs timed to start at stimulus onset. A minimum of 200 trials were acquired under each viewing condition.

Simulating the effects of disease

A key problem in determining the performance of signal detection algorithms using clinical data is uncertainty about the true effect the disease has on the recording. One of the most common effects of disease on the mfERG is the attenuation of responses. For example patients with advanced Retinitis Pigmentosa may appear to have recordings that are indistinguishable from noise to human examination but other algorithms may identify preserved responses (Gerth et al. 2007). Similarly VEP signals may be reduced due to the effects of disease, poor attention or accommodation. Equally poor compliance may increase the background noise of the recordings making signal detection more difficult.

Paper I

In this paper we used two methods to modify mfERG responses recorded from visually normal adult volunteers to simulate the effects of disease. Complete signal loss was simulated by replacing the portion of the recorded waveform that contains significant retinal responses (the signal epoch) with a separate portion of the recorded waveform that was considered to contain only responses uncorrelated with the stimulus (the noise epoch). Signal attenuation was simulated by combining a signal epoch with a noise epoch multiplied by a factor, the resultant combined epoch was then scaled to approximate the original root mean square (RMS) amplitude of the original wave (Figure 16).

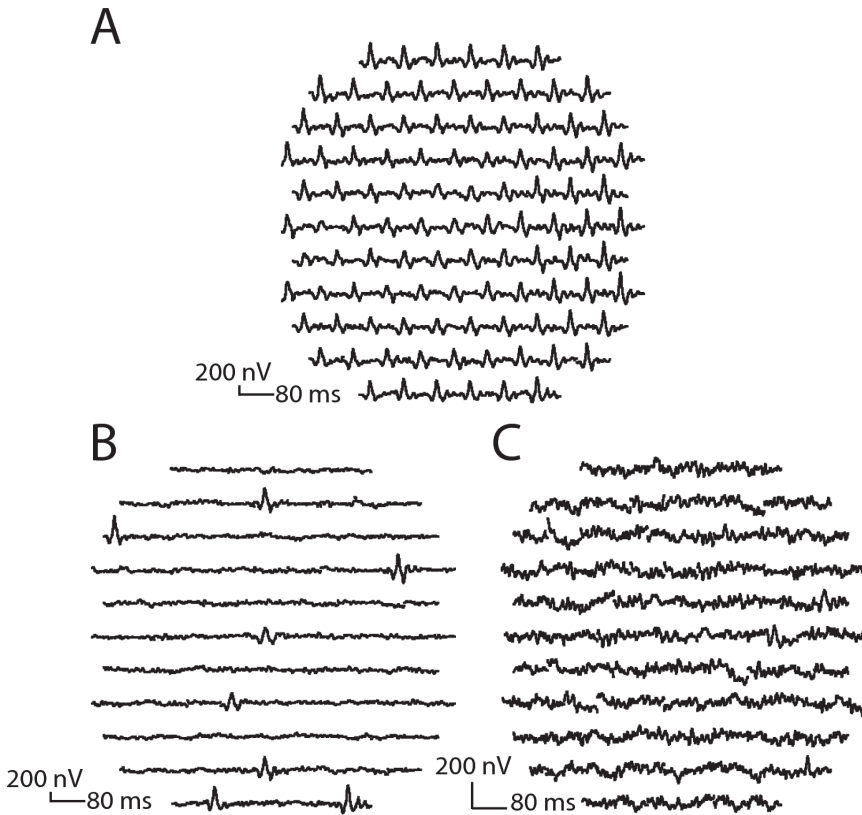


Figure 16: Post processing of an individual mfERG recording. A) The raw mfERG recording. B) Recording after removal of signal from 95 hexagons. C) The same recording after attenuation by a factor of 5. Note the difference in amplitude scales.

Paper II

In this paper we attempted to simulate both the effects of vision loss and poor compliance on VEP recordings. Vision loss was simulated by obscuring the stimulus with an opaque screen. A variety of techniques were used to simulate poor compliance, these included increasing noise due to movement and muscle artefacts as well as decreased attention by forcing the subjects to hold a conversation during the recording process.

Signal detection algorithms

Paper I

Four signal detection methods were compared. Three methods were fully automated while the fourth was manual. For the manual method, the mfERG recordings were analysed by four electrophysiologists who were asked to identify any stimulus areas that they thought contained a response. Of the three automated scoring algorithms, two were based on template matching and the third on a measure of the SNR. The two template matching algorithms relied on matching an idealised template waveform to each of the artificially modified recordings. The template was scaled in amplitude and either linearly slid along the time axis (additive scaling), or stretched on the time axis (multiplicative scaling). A good match between the scaled template and the target waveform was taken to indicate a signal was present while a poor match was taken as indicating the signal has been removed. The SNR was calculated as the root mean square (RMS) amplitude of the signal epoch / RMS of the noise epoch.

Paper II

Three signal identification algorithms were compared in this study. Instead of the response being classified as present or absent as it was in Paper I, the algorithms used in this study generated a probability that the trial contained a response. A weighted average was then calculated that assigned a higher weights to trials thought more likely to contain a response. A template matching algorithm, similar to that described for Paper I, used a template based on a published ideal VEP response. A coherence algorithm, similar to that suggested by Woody (Harris & Woody 1969) measured the similarity between different waveforms. Trials with very similar responses were considered as likely to

contain a signal, while those with a low degree of feature conservation were considered as likely containing only noise. The final algorithm used a neural network. The network was trained to recognize trials containing the VEP response and assigned a probability that the trial contained a response.

Measuring Performance

Paper I

The artificial modification of multifocal recordings means that the presence or absence of a particular signal could be known with certainty. Coupled with the boolean nature of the identification problem (either a signal is present or it is absent) allows the performance of the signal detection algorithms to be compared using measures of sensitivity and specificity.

Paper II

The use of probabilities for the signal identification algorithms used in this study precludes the use of sensitivity and specificity as outcome measures. Instead a variety of outcomes that would be useful in recording clinical VEPs were considered. These included the amplitude and SNR of the resultant waveform as well as a measure of the time taken for the resultant waveform to become significantly different from noise (Young & Kimura 2010). This later outcome measure overcomes the subjectivity required of human observers when identifying waveforms and could be of particular use when recordings are made by less experienced technicians or from less cooperative subjects.

Identifying changes to retinal function occurring as a result of disease

Paper III

The problem addressed in Paper III was the identification of subtle, sub-clinical, changes caused by Type 1 Diabetes before the onset of retinopathy. Multifocal electroretinograms were recorded from a population with Type 1 Diabetes and an age similar control population. The mfERG data were analysed using the template fitting technique described earlier, and the sf-mfERG data were

analysed using SNR. In this case the SNR was calculated as

$$\text{SNR} = (\text{RMS}_{\text{signal}} + \text{RMS}_{\text{noise}}) / \text{RMS}_{\text{noise}}$$

Responses from individual hexagons, as well as responses formed by averaging the data from equivalent eccentricities and from retinal quadrants, were compared between the two populations to investigate the spatial distribution of any identified changes.

Data were also analysed using a multivariate analysis, spatio-temporal partial least squares (st-PLS) (Krishnan et al. 2011). This interesting analytical technique enables the detection of changes in waveform shape without requiring reduction of either the spatial distribution or temporal distribution of the data. The type of st-PLS analysis used (Mean-centered task PLS) (Krishnan et al. 2011) has been used in ERP studies of memory (Bergström et al. 2007; West & Wymbs 2004; West & Kropfingger 2005) as well as fMRI studies (McIntosh & Lobaugh 2004; Martínez-Montes et al. 2004; Protzner et al. 2009).

Results and Discussion

Signal detection algorithms

The studies described in Papers I and II demonstrate that automated signal detection algorithms can increase the sensitivity and reduce the subjectivity of clinical visual electrophysiological recordings. The results of paper I show that even when mfERG signals are not attenuated artificially there is a large variation in the sensitivity of human observers. The best performing automated signal detection algorithms had a higher sensitivity than the highest performing human observer.

Effect of increasing noise

Not surprisingly the performance of all the signal detection algorithms decreased as the proportion of noise in the recorded waveforms increased. In Paper I the amount of noise was modified systematically. When the amount of noise was increased by a factor of 2, the sensitivity of the best performing algorithm (template sliding) was reduced by 9% whereas the sensitivity of the worst performing algorithm (SNR) reduced by 47%. The average reduction for human observers was 20% (Table 1 & Table 2). When the amount of noise was increased by a factor of 5 the algorithms based on template matching still performed better than chance, the SNR algorithm was unable to separate the responses containing signal from those containing only noise. Human performance at this noise level was not tested but unpublished, preliminary data indicated that performance was no better than chance. Previous work has demonstrated that an SNR based algorithm was able to detect highly attenuated signals in clinical mfERGs recorded from patients with advanced RP. When hexagons identified by the SNR metric were averaged together the distinctive mfERG waveform morphology emerged, averaging hexagons with a low SNR resulted in a waveform with a noise only morphology (Gerth et al. 2007). It would be interesting to see how well template based algorithms perform on this type of data.

Scorer	Attenuation			
	0		2	
	Sensitivity	Specificity	Sensitivity	Specificity
1	0.37	1	0.2	1
2	0.94	0.99	0.74	1
3	0.68	0.99	0.48	0.99
4	0.69	1	0.49	1

Table 1: Sensitivity and specificity for identifying signals in modified mfERG recordings for 4 human scorers.

Method	Attenuation	
	0	2
Template (additive scaling)	0.95	0.86
Template (multiplicative scaling)	0.66	0.60
SNR	0.53	0.06

Table 2: Sensitivity for automated signal detection algorithms for detecting signals in modified mfERG recordings. Sensitivity shown at 0.99 specificity level.

Although in Paper II the noise levels were not modified in a systematic manner it is still possible to draw conclusions about the performance of the template and coherence algorithms at separating signals that are contaminated with noise (condition 2) from those not containing any signal (condition 3). In this study the template matching algorithm performed almost as well at identifying contaminated trials as it did identifying trials recorded under ideal conditions. Interestingly the coherence algorithm failed to identify the contaminated trials and actually gave heavier weights to the noise only trials (Figure 17). This probably indicates that the variation in amplitude of the noise-only trials was smaller than for the trials contaminated with muscle artifact. It is not possible to draw any conclusions about the performance of the neural network algorithm since the networks were only trained to recognize the trials from condition 1.

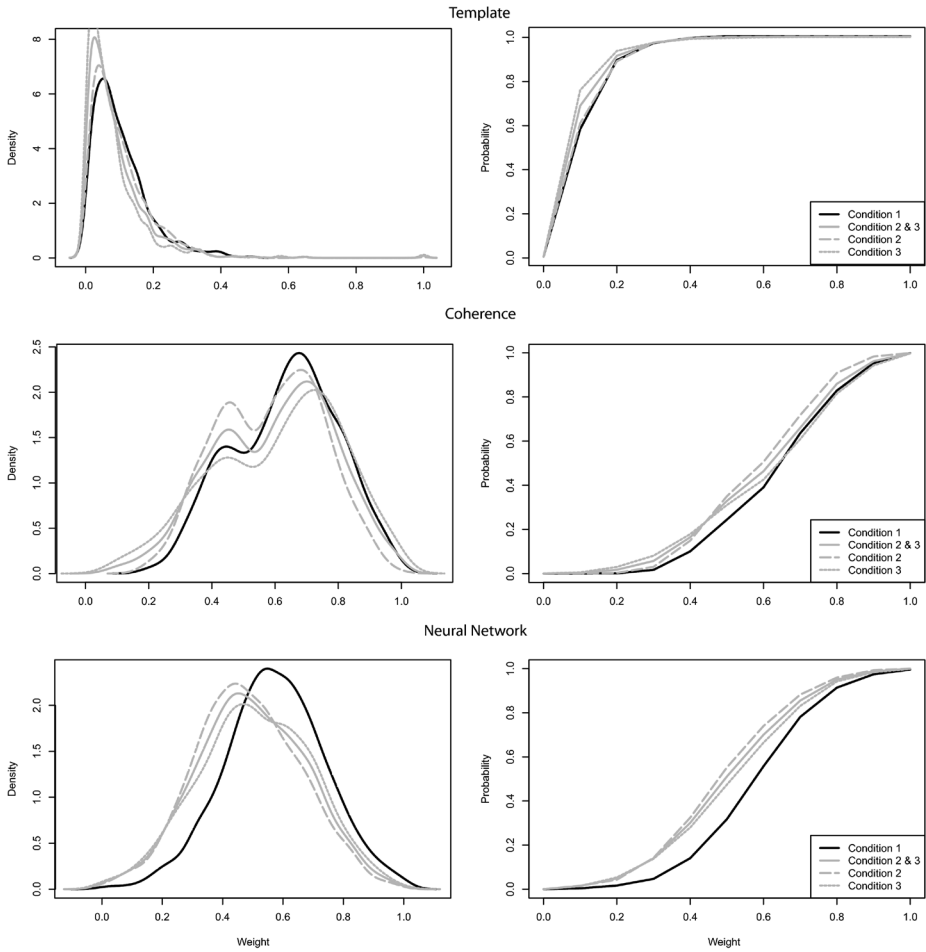


Figure 17: Weights assigned to VEP trials by automated signal detection algorithms. Weight distributions were pooled across patients. Left column shows frequency distributions, the right column shows the same data as a cumulative probability plot. Black solid line = signal epochs, gray lines = noise epochs. Dotted lines = trials with signals contaminated with noise, dashed lines = trials with no VEP response.

Effect of prior knowledge

The different signal identification algorithms all make assumptions about the waveforms. The assumptions are summarised in the table below.

Algorithm	Papers used in	Assumptions
SNR	II & III	Responses will have larger RMS amplitude than noise
Coherence	II	Underlying response is conserved between trials. More similarity between responses than noise
Template (additive scaling)	I	Morphology of response will be similar to the chosen template. Changes in timing will affect all response components identically.
Template (multiplicative scaling)	I, II & III	Morphology of response will be similar to chosen template. Changes in timing will affect later response components more than earlier response components.
Neural Network	II	Responses will have similar morphology to those used to train the networks.
Human scoring	I	Responses will be recognizable, the exact range of recognized response morphologies will be dependent on the experiences of the observer.

Table 3: Summary of assumptions made by different signal identification algorithms.

The performance of the different signal detection algorithms is dependent on the changes that occur in the recorded waveforms, for example in Paper I we showed that the SNR algorithm is more affected by signal attenuation than either of the template algorithms. In general as the signal becomes more

attenuated the algorithms that employ the most prior knowledge about the morphology of the response perform better. While this observation can be used to improve the performance of the different algorithms when the expected changes to the response are known (for example multiplicative scaling was found to better represent the changes to the mfERG due to Diabetes than additive scaling (Schneck et al. 2004)), often the underlying changes are unknown and preliminary investigations will be necessary.

When a template waveform is required it is important that the template waveform be representative of the expected response. Since the morphology of the waveforms change as the underlying physiological systems mature (Westall et al. 1999; Taylor & McCulloch 1992; Seiple 2003) it is important that the age of the subject is taken into account when selecting the template. The ISCEV Standards for Clinical Multifocal Electrophysiology suggest the template should be generated from age-matched normal data (Hood et al. 2012), there is however a possibility that the template could be over specified, becoming less sensitive to variations in waveforms caused by population variation or by disease. Other template based analyses have shown success using templates that are much less specific to the expected waveform (Simpson et al. 2009). It is interesting to note that the template analysis used in Paper III, used templates specific for each stimulated area in the mfERG. As a result the analysis was insensitive to the variations of the waveform that occur across the retina (Baseler et al. 1994).

Identifying changes due to disease

In Paper III patients with Type 1 Diabetes, before the onset of clinical retinopathy, were studied to identify changes in the mfERG responses. The multiplicative scaling template matching technique identified a delay corresponding to a 0.2 ms delay in the P1 component of the waveform. The same delay was identified when individual hexagon responses, ring averaged responses and quadrant averaged responses were analysed. This finding is similar to that of other groups (Schneck et al. 2004), however, it has not been possible to localise this delay to any particular retinal area. The SNR analysis of the sf-mfERG recordings was not able to identify any difference between the two groups although these differences have been observed using other analysis techniques (Bears et al. 2004; Kurtenbach et al. 2000).

The multivariate st-PLS analysis was also able to identify a significant delay in the responses of the subjects with Diabetes. Examination of the response waveforms indicated that this delay spread across the whole retina, with the least amount of delay being observed in the inferior nasal retinal quadrant. The st-PLS analysis also indicated that both the leading and falling edge of the main P1 component were affected (Figure 18). While it is unclear why different parts of the waveform should be affected in different retinal areas, it is known that the rising edge represents the interaction of depolarising ON-bipolar cells and the recovery of the OFF-bipolar cells, while the trailing edge is the interaction of depolarisation of the OFF-bipolar cells and the recovery of the ON-bipolar cells (Hood et al. 2002). It is possible that the temporal distribution of the identified changes may give clues about the retinal cell types that are affected.

The st-PLS analysis was more sensitive than the SNR analysis and was able to identify a significant difference in the sf-mfERG results. Examination of the distribution of the differences showed that the difference manifested as a delay in the response, to which the SNR analysis was not sensitive. Although previous studies have also observed this delay, they have used spatial averaging of the mfERG data and in order to draw conclusions about the distribution of these delays the averaging scheme, which matched the distribution of the changes had to be selected (Kurtenbach et al. 2000). As st-PLS does not require any reduction of the spatial distribution of the data it was able to study the response delays on an individual hexagon basis. While the delays are distributed across the whole tested retinal area, they seemed to concentrate in a parafoveal ring which is where the nerve fibre layer is thickest.

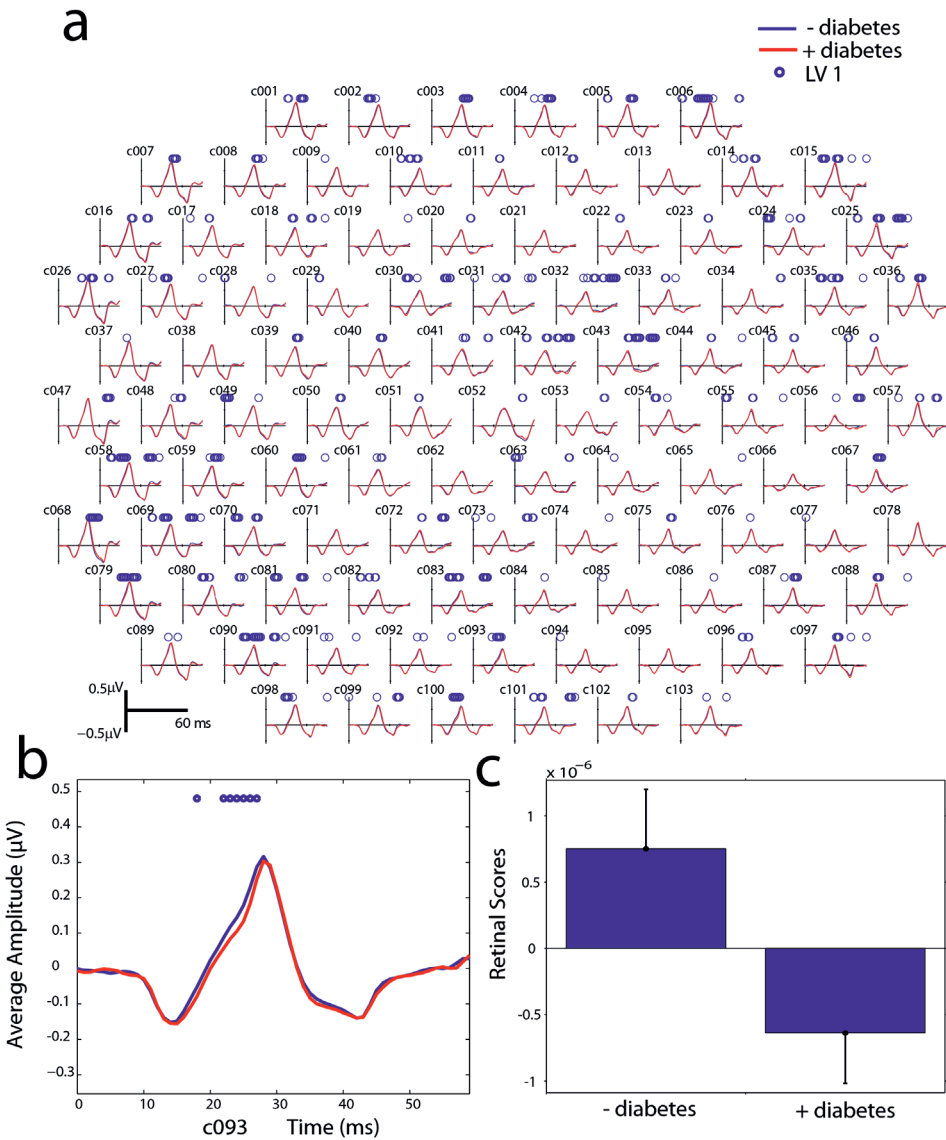


Figure 18: Partial least-squares analysis of mfERGs. a) Group average standard mfERG waveforms. Average mfERG waveforms from 103 retinal areas are shown. Red lines are the average waveform from subjects with Diabetes and blue lines are the average from control subjects. Circles above the waveforms indicate time points that are significantly different between groups. **b)** close-up from a hexagon in the inferior retina (c093) with significant time points on the rising edge of PI. **c)** retina response scores for LV1 associated with the 2 groups.

Limitations

While the artificial simulation of disease promises to be a powerful approach for measuring the performance of novel analysis techniques, it is important that the techniques used replicate the expected disease processes. The techniques used in Paper I were limited to modifying the relative amplitudes of signal and noise, there was no attempt to alter the timing of the response. While changes to mfERG amplitude are common, delays in mfERG timing have also been observed. It is possible that if timing delays are present the relative performance of the algorithms may change.

In Paper II the effect of a non-compliant patient was simulated. The techniques used simulated the effect of increased artifactual noise and decreased signal due to inattention. While these are realistic problems encountered in clinical testing, diseases, such as seizure disorders, may have other effects on the underlying brain activity or response morphology, which were not tested in this study. The most common changes to the VEP, due to disease, are changes in the timing of the response. So long as the gross morphology of the waveform does not change the algorithms used should be equally effective.

The metrics used to measure the performance of the algorithms used in Papers I and II concentrated on their ability to detect electrophysiological signals, no attempt was made to quantify their ability to determine the response morphology. Other studies have shown that automated algorithms can outperform human observers in describing the underlying response in the presence of noise accurately (Fisher et al. 2007).

The st-PLS analysis pools the data with groups and uses this pooled data to determine the statistical significance of any changes. It is not possible to use this method to determine statistically significant changes occurring in a single recording from a single patient. This limits the clinical applicability. However the additional information about the morphology and spatial distribution of the changes can be used to guide the choice of other analysis techniques that are more suitable for use on single sample data.

The difficulties encountered in accurately simulating the effects of disease only strengthen the argument that metrics of signal quality and reliability should be incorporated into visual electrophysiology testing.

Conclusions

Paper I

Automated algorithms can be used for signal detection in mfERG recordings.

Automated algorithms could outperform human experts in terms of sensitivity and specificity for signal detection.

Algorithms with better prior knowledge of expected waveform shape outperformed naive algorithms.

The optimal algorithm (Template with additive scaling) achieved a sensitivity of 86% at 99% specificity for detecting attenuated responses. The best human observer achieved sensitivity of 74% using the same data.

Paper II

Automated signal detection algorithms coupled with weighted averaging were able to improve the quality and reduce the time required for recording VEPs.

A neural network algorithm, on average, gave trials containing VEP responses a 14% higher weighting than trials that contained no VEP response.

All the automated algorithms reduced the time taken to obtain a statistically significant algorithm compared with traditional ensemble averaging. A coherence algorithm that looked for similarity between trials required only 25% of the trials to achieve a significant response.

Paper III

Changes to retinal function, occurring in a population with Type 1 Diabetes before clinical retinopathy, were identified both by a template matching (multiplicative scaling) and by multivariate st-PLS analysis. Spatial-temporal PLS analysis was able to identify changes to the slopes of the responses that are usually lost with other analysis techniques. This additional information may provide clues to the underlying physiological processes that are disturbed in the retinae of patients with Type 1 Diabetes.

Summary

The use of advanced algorithms for signal identification and analysis shows promise for both increasing the sensitivity and reducing the subjectivity of visual electrophysiological recordings. The reduced subjectivity may aid the sharing of results between electrophysiology laboratories and with other related disciplines.

Acknowledgements

There are many people I need to thank for making this work possible.

My supervisors:

Carol Westall gave me the opportunity to achieve as much as I wanted and Josefin Nilsson who pushed me to achieve slightly more.

My colleagues in the VEU, Carole Panton and Melissa Cotesta, whose knowledge, support and humour has been invaluable.

Other staff and students particularly Fil Cortese and Christina Gerth, in the Department of Ophthalmology at the Hospital for Sick Children, for providing ideas and support.

To my family Caroline, Oscar and Molly who have put up with so much and made this all possible I can only offer my love and gratitude.

Finally my parents, teachers and everyone else who have demonstrated that learning is not a product of schooling but the lifelong attempt to acquire it (Albert Einstein 1879 - 1955).

References

- Almoqbel, F., Leat, S.J. & Irving, E., 2008. The technique, validity and clinical use of the sweep VEP. *Ophthalmic & physiological optics : the journal of the British College of Ophthalmic Opticians (Optometrists)*, 28(5), pp.393-403.
- Apkarian, P. et al., 1983. A decisive electrophysiological test for human albinism. *Electroencephalography and clinical neurophysiology*, 55(5), pp.513-31.
- Apkarian, P. & Bour, L.J., 2006. Aberrant albino and achiasmat visual pathways: Noninvasive Electrophysiological Assessment. In J. R. Heckenlively & G. B. Arden, eds. *Principals and practice of clinical electrophysiology of vision2*. Cambridge, MA.: MIT Press, pp. 369-398.
- Arieli, A. et al., 1996. Dynamics of ongoing activity: explanation of the large variability in evoked cortical responses. *Science*, 273(5283), pp.1868-1871.
- Armington, J.C., 1974. *The Electroretinogram*, New York: Academic Press.
- Audo, I. et al., 2008. The negative ERG: clinical phenotypes and disease mechanisms of inner retinal dysfunction. *Survey of ophthalmology*, 53(1), pp.16-40.
- Baseler, H.A. et al., 1994. The topography of visual evoked response properties across the visual field. *Electroencephalography and clinical neurophysiology*, 90(1), pp.65-81.
- Bearse, M.A. et al., 2004. Local multifocal oscillatory potential abnormalities in diabetes and early diabetic retinopathy. *Invest Ophthalmol Vis Sci*, 45(9), pp.3259-3265.
- Bech-Hansen, N.T. et al., 1998. Loss-of-function mutations in a calcium-channel alpha1-subunit gene in Xp11.23 cause incomplete X-linked congenital stationary night blindness. *Nature genetics*, 19(3), pp.264-7.
- Bech-Hansen, N.T. et al., 2000. Mutations in NYX, encoding the leucine-

- rich proteoglycan nyctalopin, cause X-linked complete congenital stationary night blindness. *Nature genetics*, 26(3), pp.319-23.
- Bergström, Z.M. et al., 2007. ERP evidence for successful voluntary avoidance of conscious recollection. *Brain research*, 1151, pp.119-33.
- Berson, E.L., 1993. Retinitis pigmentosa. The Friedenwald Lecture. *Investigative ophthalmology & visual science*, 34(5), pp.1659-76.
- Berson, E.L., 1996. Retinitis pigmentosa: unfolding its mystery. *Proceedings of the National Academy of Sciences of the United States of America*, 93(10), pp.4526-8.
- Birch, D.G., 2006. Retinitis Pigmentosa. In *Principals and practice of clinical electrophysiology of vision*. Cambridge, MA.: MIT Press, pp. 781-794.
- Burns, M.E. & Lamb, T.D., 2004. Visual Transduction by Rod and Cone Photoreceptors. In L. M. Chalupa & J. S. Werner, eds. *The Visual Neurosciences2*. Cambridge, MA.: MIT Press, pp. 215-233.
- Cioffi, G.A., Elisabet, G. & Alm, A., 2003. Ocular Circulation. In P. L. Kaufman & A. Alm, eds. *Adler's Physiology Of The Eye*. St. Louis, MO, USA: Mosby, pp. 747-784.
- Coupland, S.G., 2006. Electrodes for Visual Testing. In J. R. Heckenlively & G. B. Arden, eds. *Principals and practice of clinical electrophysiology of vision*. Cambridge, MA.: The MIT Press, pp. 245-254.
- Cuypers, M.H. & Thijssen, J.M., 1995. Improving the ensemble average of visual evoked potentials. II. Simulations and experiments. *Technology and health care: official journal of the European Society for Engineering and Medicine*, 3(1), pp.33-42.
- Dacey, D.M., 1999. Primate retina: cell types, circuits and color opponency. *Progress in retinal and eye research*, 18(6), pp.737-63.
- Dawson, G.D., 1947. CEREBRAL RESPONSES TO ELECTRICAL STIMULATION OF PERIPHERAL NERVE IN MAN. *Journal of neurology, neurosurgery, and psychiatry*, 10(3), pp.134-40.
- Delori, F.C. et al., 1995. In vivo measurement of lipofuscin in Stargardt's

disease--Fundus flavimaculatus. *Investigative ophthalmology & visual science*, 36(11), pp.2327-31.

- Dolan, F.M. et al., 2002. The wide field multifocal electroretinogram reveals retinal dysfunction in early retinitis pigmentosa. *The British journal of ophthalmology*, 86(4), pp.480-1.
- Dustman, R.E. et al., 1977. The cerebral evoked potentials: Life span change and twin studies. In J. E. Desmedt, ed. *Visual Evoked Potentials in Man*. Oxford: Clarendon, pp. 363-377.
- Emmerson-Hanover, R. et al., 1994. Pattern reversal evoked potentials: gender differences and age-related changes in amplitude and latency. *Electroencephalography and clinical neurophysiology*, 92(2), pp.93-101.
- Van Essen, D.C., Anderson, C.H. & Felleman, D.J., 1992. Information processing in the primate visual system: an integrated systems perspective. *Science (New York, N.Y.)*, 255(5043), pp.419-23.
- Fahrenfort, I. et al., 2005. The involvement of glutamate-gated channels in negative feedback from horizontal cells to cones. *Progress in brain research*, 147, pp.219-29.
- Falk, G. & Shells, R., 2006. Synaptic Transmission: Sensitivity Control Mechanisms. In J. R. Heckenlively & G. B. Arden, eds. *Principals and practice of clinical electrophysiology of vision*. Cambridge, MA.: The MIT Press, pp. 79-91.
- Fisher, A.C., Hagan, R.P. & Brown, M.C., 2007. Automatic positioning of cursors in the transient pattern electroretinogram (PERG) with very poor SNR using an Expert System. *Documenta ophthalmologica. Advances in ophthalmology*, 115(2), pp.61-8.
- Foley J.D. et al., 1996. *Computer Graphics: Principles and Practice* 2nd ed., Addison-Wesley.
- Frederiksen, J.L. & Petreera, J., 1999. Serial visual evoked potentials in 90 untreated patients with acute optic neuritis. *Survey of ophthalmology*, 44 Suppl 1(October), pp.S54-62.
- Friston, K.J., Frith, C.D. & Frackowiak, R.S.J., 1993. Principal Component Analysis Learning Algorithms: A Neurobiological Analysis. *Proceedings of the Royal Society B: Biological Sciences*,

254(1339), pp.47-54.

- Garey, L.J., 2006. *Localisation in the Cerebral Cortex*, New York, NY, USA: Springer.
- Gerth, C. et al., 2007. Assessment of central retinal function in patients with advanced retinitis pigmentosa. *Invest Ophthalmol Vis Sci*, 48(3), pp.1312-1318.
- Granit, R., 1933. The components of the retinal action potential in mammals and their relation to the discharge in the optic nerve. *The Journal of physiology*, 77(3), pp.207-39.
- Gregori, B. et al., 2006. Vep latency: Sex and head size. *Clinical Neurophysiology*, 117(5), pp.1154-1157.
- Haig, A.R. et al., 1995. Classification of single-trial ERP sub-types: application of globally optimal vector quantization using simulated annealing. *Electroencephalogr Clin Neurophysiol*, 94(4), pp.288-297.
- Harris, E. & Woody, C., 1969. Use of an adaptive filter to characterize signal-noise relationships. *Computers and Biomedical Research*, 2(3), pp.242-273.
- Harter, M.R. & White, C.T., 1970. Evoked cortical responses to checkerboard patterns: effect of check-size as a function of visual acuity. *Electroencephalography and clinical neurophysiology*, 28(1), pp.48-54.
- von Helmholtz, H., 1909. *Handbook of Physiological Optics* Electronic. J. P. C. Southall, ed., Optical Society of America.
- Holmes, G., 1945. Ferrier Lecture: the organization of the visual cortex in man. *Proceedings of the Royal Society of London. Series B*, 361(1476), pp.2239-59.
- Hood, D. & Li, J., 1997. A technique for measuring individual multifocal ERG records. *Trends Opt Photon*, 11, pp.280-293.
- Hood, D.C. et al., 2012. ISCEV standard for clinical multifocal electroretinography (mfERG) (2011 edition). *Documenta ophthalmologica. Advances in ophthalmology*, 124(1), pp.1-13.
- Hood, D.C. et al., 2002. Retinal origins of the primate multifocal ERG:

- implications for the human response. *Invest Ophthalmol Vis Sci*, 43(5), pp.1673-1685.
- Hood, D.C. & Finkelstein, M.A., 1986. Visual Sensitivity. In K. R. Boff, L. Kaufman, & J. P. Thomas, eds. *Handbook of Perception and Human Performance* 1. New York: Wiley.
- Hoyt, C.S., 1984. The clinical usefulness of the visual evoked response. *Journal of pediatric ophthalmology and strabismus*, 21(6), pp.231-4.
- Ihrke, M., Schrobsdorff, H. & Herrmann, J.M.M., 2009. Denoising and averaging techniques for electrophysiological data. *Coordinated Activity in the Brain*, 2, pp.165–189.
- Itier, R.J., Taylor, M.J. & Lobaugh, N.J., 2004. Spatiotemporal analysis of event-related potentials to upright, inverted, and contrast-reversed faces: effects on encoding and recognition. *Psychophysiology*, 41(4), pp.643-53.
- Jacobs, G.H., 1969. Receptive fields in visual systems. *Brain research*, 14(3), pp.553-73.
- James, C.J. & Hesse, C.W., 2005. Independent component analysis for biomedical signals. *Physiological Measurement*, 26(1), p.R15-R39.
- Jasper, H.H., 1958. The ten-twenty electrode system of the International Federation. *Electroencephalography and clinical neurophysiology*, 10, p.370.
- Jung, T., Bader, N. & Grune, T., 2007. Lipofuscin: formation, distribution, and metabolic consequences. *Annals of the New York Academy of Sciences*, 1119, pp.97-111.
- Kamermans, M. & Spekreijse, H., 1999. The feedback pathway from horizontal cells to cones. A mini review with a look ahead. *Vision Res*, 39(15), pp.2449-2468.
- Klem, G.H. et al., 1999. The ten-twenty electrode system of the International Federation. The International Federation of Clinical Neurophysiology. *Electroencephalography and clinical neurophysiology. Supplement*, 52, pp.3-6.
- Kline, R.P., Ripps, H. & Dowling, J.E., 1978. Generation of b-wave

- currents in the skate retina. *Proceedings of the National Academy of Sciences of the United States of America*, 75(11), pp.5727-31.
- Klistorner, A. et al., 2008. Correlation between full-field and multifocal VEPs in optic neuritis. *Documenta ophthalmologica. Advances in ophthalmology*, 116(1), pp.19-27.
- Knuth, K.H. et al., 2006. Differentially variable component analysis: Identifying multiple evoked components using trial-to-trial variability. *Journal of neurophysiology*, 95(5), pp.3257-76.
- Kolb, H., 1997. Amacrine cells of the mammalian retina: neurocircuitry and functional roles. *Eye (London, England)*, 11 (Pt 6), pp.904-23.
- Kondo, M. et al., 2001. Multifocal ERG findings in complete type congenital stationary night blindness. *Investigative ophthalmology & visual science*, 42(6), pp.1342-8.
- Krishnan, A. et al., 2011. Partial Least Squares (PLS) methods for neuroimaging: A tutorial and review. *Neuroimage*, 56(2), pp.455-475.
- Kurtenbach, A., Langrova, H. & Zrenner, E., 2000. Multifocal oscillatory potentials in type 1 diabetes without retinopathy. *Invest Ophthalmol Vis Sci*, 41(10), pp.3234-3241.
- Lachapelle, P. & Benoit, J., 1994. Interpretation of the filtered 100- to 1000-Hz electroretinogram. *Documenta ophthalmologica. Advances in ophthalmology*, 86(1), pp.33-46.
- Lange, D.H. et al., 2000. Overcoming selective ensemble averaging: unsupervised identification of event-related brain potentials. *IEEE Trans Biomed Eng*, 47(6), pp.822-826.
- Lawwill, T. & Burian, H.M., 1966. A modification of the Burian-Allen contact-lens electrode for human electroretinography. *American journal of ophthalmology*, 61(6), pp.1506-9.
- Lei, B. & Perlman, I., 1999. The contributions of voltage- and time-dependent potassium conductances to the electroretinogram in rabbits. *Visual neuroscience*, 16(4), pp.743-54.
- Levin, A.V. & Stroh, E., 2011. Albinism for the busy clinician. *Journal of AAPOS: the official publication of the American Association for*

Pediatric Ophthalmology and Strabismus / American Association for Pediatric Ophthalmology and Strabismus, 15(1), pp.59-66.

- Lodha, N., 2007. *Objective and Subjective Visual Functions in Stargardt Macular Dystrophy*. University of Toronto.
- Lukasiewicz, P.D., 2005. Synaptic mechanisms that shape visual signaling at the inner retina. *Progress in brain research*, 147, pp.205-18.
- Mackay, A.M. et al., 2008. Real-time rapid acuity assessment using VEPs: development and validation of the step VEP technique. *Investigative ophthalmology & visual science*, 49(1), pp.438-41.
- Mackie, R.T. et al., 1995. Comparison of visual assessment tests in multiply handicapped children. *Eye (London, England)*, 9 (Pt 1), pp.136-41.
- Malcolm, C.A., McCulloch, D.L. & Shepherd, A.J., 2007. Pattern-reversal visual evoked potentials in infants: gender differences during early visual maturation. *Developmental medicine and child neurology*, 44(5), pp.345-351.
- Mansergh, F. et al., 2005. Mutation of the calcium channel gene *Cacna1f* disrupts calcium signaling, synaptic transmission and cellular organization in mouse retina. *Human molecular genetics*, 14(20), pp.3035-46.
- Marmor, M.F. et al., 2009. ISCEV Standard for full-field clinical electroretinography (2008 update). *Documenta ophthalmologica. Advances in ophthalmology*, 118(1), pp.69-77.
- Marmor, M.F. et al., 2011. ISCEV standard for clinical electro-oculography (2010 update). *Documenta ophthalmologica. Advances in ophthalmology*, 122(1), pp.1-7.
- Martínez-Montes, E. et al., 2004. Concurrent EEG/fMRI analysis by multiway Partial Least Squares. *NeuroImage*, 22(3), pp.1023-34.
- Masic, N. & Pfurtscheller, G., 1993. Neural network based classification of single-trial EEG data. *Artificial Intelligence in Medicine*, 5(6), pp.503-513.
- Masland, R.H., 2001. The fundamental plan of the retina. *Nature*

- neuroscience*, 4(9), pp.877-86.
- Mason, C. & Erskine, L., 2004. The development of Retinal Decussations. In L. M. Chalupa & J. S. Werner, eds. *The Visual Neurosciences*. Cambridge, MA.: MIT Press, pp. 94-107.
- McIntosh, A.R. et al., 1996. Spatial pattern analysis of functional brain images using partial least squares. *Neuroimage*, 3(3 Pt 1), pp.143-157.
- McIntosh, A.R. & Lobaugh, N.J., 2004. Partial least squares analysis of neuroimaging data: applications and advances. *NeuroImage*, 23 Suppl 1, pp.S250-63.
- Meigen, T. & Bach, M., 1999. On the statistical significance of electrophysiological steady-state responses. *Documenta ophthalmologica. Advances in ophthalmology*, 98(3), pp.207-32.
- Mentzer, A.E. et al., 2005. Influence of recording electrode type and reference electrode position on the canine electroretinogram. *Documenta ophthalmologica. Advances in ophthalmology*, 111(2), pp.95-106.
- Miyake, Y., 2006. Congenital Stationary Night Blindness. In J. R. Heckenlively & G. B. Arden, eds. *Principals and practice of clinical electrophysiology of vision2*. Cambridge, MA.: MIT Press, pp. 829-840.
- Miyake, Y. et al., 1986. Congenital stationary night blindness with negative electroretinogram. A new classification. *Archives of ophthalmology*, 104(7), pp.1013-20.
- Moeller, J., Strother, S. & Sidtis, J., 1987. Scaled Subprofile Model: A Statistical Approach to the Analysis of Functional Patterns in Positron Emission Tomographic Data. *Journal of Cerebral*, pp.649-658.
- Möcks, J. et al., 1987. Trial-to-trial variability of single potentials: methodological concepts and results. *The International journal of neuroscience*, 33(1-2), pp.25-32.
- NIH, Retinitis pigmentosa. *Genetic and Rare Diseases Information Center (GARD)*.

- Naismith, R.T. et al., 2009. Optical coherence tomography is less sensitive than visual evoked potentials in optic neuritis. *Neurology*, 73(1), pp.46-52.
- Najafabadi, F.S., Zahedi, E. & Mohd Ali, M.A., 2006. Fetal heart rate monitoring based on independent component analysis. *Computers in biology and medicine*, 36(3), pp.241-52.
- Nelson, R., 1982. All amacrine cells quicken time course of rod signals in the cat retina. *Journal of neurophysiology*, 47(5), pp.928-47.
- Nelson, R. & Connaughton, V., 1995. Bipolar Cell Pathways in the Vertebrate Retina. *Webvision*.
- Odom, J.V. et al., 2010. ISCEV standard for clinical visual evoked potentials (2009 update). *Documenta ophthalmologica. Advances in ophthalmology*, 120(1), pp.111-9.
- Odom, J.V. et al., 1987. Pattern electroretinogram: effects of reference electrode position. *Documenta ophthalmologica. Advances in ophthalmology*, 65(3), pp.297-306.
- Odom, J.V. et al., 2004. Visual evoked potentials standard (2004). *Documenta ophthalmologica. Advances in ophthalmology*, 108(2), pp.115-23.
- Pau, D. et al., 2011. Optic neuritis. *Eye (London, England)*, 25(7), pp.833-42.
- Protzner, A.B. et al., 2009. The temporal interaction of modality specific and process specific neural networks supporting simple working memory tasks. *Neuropsychologia*, 47(8-9), pp.1954-63.
- Rangaswamy, N.V. et al., 2007. Effects of Spectral Characteristics of Ganzfeld Stimuli on the Photopic Negative Response (PhNR) of the ERG. *Investigative ophthalmology & visual science*, 48(10), pp.4818-28.
- Regan, D., 1989. Technical and Mathematical Considerations. In *Human Brain Electrophysiology*. New York, NY, USA: Elsevier Science Publishing Co. Inc., pp. 1-155.
- Risner, M.L. et al., 2009. The Visual Evoked Potential is independent of surface alpha rhythm phase. *NeuroImage*, 45(2), pp.463-9.

- Rossi, E.A. et al., 2007. Visual performance in emmetropia and low myopia after correction of high-order aberrations. *Journal of vision*, 7(8), p.14.
- Rousseau, S. & Lachapelle, P., 1999. The electroretinogram recorded at the onset of dark-adaptation: understanding the origin of the scotopic oscillatory potentials. *Documenta ophthalmologica. Advances in ophthalmology*, 99(2), pp.135-50.
- Schiller, P.H., 2010. Parallel information processing channels created in the retina. *Proceedings of the National Academy of Sciences of the United States of America*, 107(40), pp.17087-94.
- Schimmel, H., 1967. The (\pm) reference: accuracy of estimated mean components in average response studies. *Science*, 157(3784), p.92.
- Schmidt, T.M. et al., 2011. Melanopsin-positive intrinsically photosensitive retinal ganglion cells: from form to function. *The Journal of neuroscience: the official journal of the Society for Neuroscience*, 31(45), pp.16094-101.
- Schneck, M.E. et al., 2004. Comparison of mfERG waveform components and implicit time measurement techniques for detecting functional change in early diabetic eye disease. *Doc Ophthalmol*, 108(3), pp.223-230.
- Schubert, G. & Bornschein, H., 1952. [Analysis of the human electroretinogram]. *Ophthalmologica. Journal international d'ophthalmologie. International journal of ophthalmology. Zeitschrift für Augenheilkunde*, 123(6), pp.396-413.
- Seiple, W., 2003. Multifocal Electroretinography as a Function of Age: The Importance of Normative Values for Older Adults. *Investigative Ophthalmology & Visual Science*, 44(4), pp.1783-1792.
- Sherman, S.M., 2001. Thalamic relay functions. *Progress in brain research*, 134, pp.51-69.
- Simpson, D.M. et al., 2009. Objective Methods for the Detection of Pattern Electroretinograms (PERG). In *World Congress on Medical Physics and Biomedical Engineering, September 7-12, 2009, Munich, Germany*. Springer, pp. 156–159.
- Skarf, B. & Panton, C.M., 1987. VEP testing in neurologically impaired

and developmentally delayed infants and young children. *Investigative ophthalmology & visual science*, 28(suppl), p.302.

Slaughter, M.M. & Miller, R.F., 1981. 2-amino-4-phosphonobutyric acid: a new pharmacological tool for retina research. *Science (New York, N.Y.)*, 211(4478), pp.182-5.

Smith, W.C., 2006. Phototransduction and Photoreceptor Physiology. In J. R. Heckenlively & G. B. Arden, eds. *Principals and practice of clinical electrophysiology of vision*. Cambridge, MA.: MIT Press, pp. 65-77.

Soong, F., Levin, a V. & Westall, C. a, 2000. Comparison of techniques for detecting visually evoked potential asymmetry in albinism. *Journal of AAPOS: the official publication of the American Association for Pediatric Ophthalmology and Strabismus / American Association for Pediatric Ophthalmology and Strabismus*, 4(5), pp.302-10.

Sutter, E.E., 2001. Imaging visual function with the multifocal m-sequence technique. *Vision research*, 41(10-11), pp.1241-55.

Sutter, E.E. & Tran, D., 1992. The field topography of ERG components in man--I. The photopic luminance response. *Vision research*, 32(3), pp.433-46.

Taylor, M.J. & McCulloch, D.L., 1992. Visual evoked potentials in infants and children. *Journal of Clinical Neurophysiology*, 9(3), p.357.

Thie, J. et al., 2012. Gaussian wavelet transform and classifier to reliably estimate latency of multifocal visual evoked potentials (mfVEP). *Vision research*, 52(1), pp.79-87.

Trick, G.L. et al., 1984. Power spectral analysis of visual evoked potentials in multiple sclerosis. *Current eye research*, 3(10), pp.1179-86.

Velde, M. van de, 2000. *Signal Validation in Electroencephalography Research*.

Verweij, J., Kamermans, M. & Spekreijse, H., 1996. Horizontal cells feed back to cones by shifting the cone calcium-current activation range. *Vision research*, 36(24), pp.3943-53.

- Victor, J.D. & Mast, J., 1991. A new statistic for steady-state evoked potentials. *Electroencephalography and clinical neurophysiology*, 78(5), pp.378-88.
- Vincent, a, 1992. Methods for improving the signal-to-noise ratio of endogenous-evoked potentials. *Integrative physiological and behavioral science: the official journal of the Pavlovian Society*, 27(1), pp.54-65.
- Viswanathan, S. et al., 1999. The photopic negative response of the macaque electroretinogram: reduction by experimental glaucoma. *Investigative ophthalmology & visual science*, 40(6), pp.1124-36.
- Wachtmeister, L., 1987. Basic research and clinical aspects of the oscillatory potentials of the electroretinogram. *Documenta ophthalmologica. Advances in ophthalmology*, 66(3), pp.187-94.
- West, R. & Kropfing, J., 2005. Neural correlates of prospective and retrospective memory. *Neuropsychologia*, 43(3), pp.418-33.
- West, R. & Wymbs, N., 2004. Is detecting prospective cues the same as selecting targets? An ERP study. *Cognitive, affective & behavioral neuroscience*, 4(3), pp.354-63.
- Westall, C.A., Panton, C.M. & Levin, A.V., 1999. Time courses for maturation of electroretinogram responses from infancy to adulthood. *Documenta ophthalmologica. Advances in ophthalmology*, 96(4), pp.355-79.
- Wiesel, T.N., Hubel, D.H. & Lam, D.M., 1974. Autoradiographic demonstration of ocular-dominance columns in the monkey striate cortex by means of transneuronal transport. *Brain research*, 79(2), pp.273-9.
- Woody, C., 1967. Characterization of an adaptive filter for the analysis of variable latency neuroelectric signals. *Medical and Biological Engineering and Computing*, 5(6), pp.539-554.
- Xu, X. & Karwoski, C., 1995. Current source density analysis of the electroretinographic d wave of frog retina. *Journal of neurophysiology*, 73(6), pp.2459-69.
- Young, R.S.L. & Kimura, E., 2010. Statistical test of VEP waveform equality. *Documenta ophthalmologica. Advances in ophthalmology*,

120(2), pp.121-35.

- Zhang, X. et al., 2002. A signal-to-noise analysis of multifocal VEP responses: an objective definition for poor records. *Documenta ophthalmologica. Advances in ophthalmology*, 104(3), pp.287-302.
- Zhang, X. & Hood, D.C., 2004. Increasing the sensitivity of the multifocal visual evoked potential (mfVEP) technique: incorporating information from higher order kernels using a principal component analysis method. *Documenta ophthalmologica. Advances in ophthalmology*, 108(3), pp.211-22.
- Zhou, W. et al., 2007. Oscillatory potentials of the slow-sequence multifocal ERG in primates extracted using the Matching Pursuit method. *Vision research*, 47(15), pp.2021-36.
- Zieve, D. & Lusby, F.W., 2011. Optic neuritis. *A.D.A.M. Medical Encyclopedia*.